Role of mitochondrial AKAPs and heart-gut axis in cardiovascular diseases

PhD Thesis

Stefania D'Apice

"Life is not easy for any of us. But what of that? We must have perseverance and, above all, confidence in ourselves. We must believe that we are gifted for something, and that this thing, at whatever cost, must be attained."

Marie Curie

Role of mitochondrial AKAPs and heart-gut axis in cardiovascular diseases

PhD Thesis

Stefania D'Apice

13/04/1992 Caserta

(Italy)

Promotor: Prof. Perrino Cinzia

Co-Promotor: Dr. Coretti Lorena

Naples 21/3/2023

University Federico II of Naples, Faculty of Medicine, Via Pansini n. 5, 80131 Naples, Italy

List of contents

Part IV. **Discussion and conclusions**

Chapter 1

General introduction and outline of the thesis

Cardiovascular disease (CVD) is the leading cause of mortality, morbidity, and hospitalization in industrialized countries. Continuous scientific progress is essential for understanding the molecular, pathophysiological, and adaptive mechanisms underlying the development of CVD. Knowledge of these processes is fundamental to optimize the therapeutic approach, identify new potential drug targets and improve the quality of life of patients affected by CVD. Mitochondrial dysfunction, in cardiomyocyte, is among the earliest and most common molecular alterations detected in numerous CVD, frequently associated with an increase in cellular oxidative stress[1,2]. Second messenger cyclic adenosine monophosphate (cAMP) is a crucial regulator of mitochondrial function, involved in mitochondrial respiration, dynamics, reactive oxygen species (ROS) production, cell survival and death through the activation of cAMP-dependent protein kinase A (PKA). Several members of the large family of mitochondria A kinase anchor proteins (mitochondrial AKAPs) locally amplify cAMP/PKA signaling to mitochondria, regulating cardiac functions under both physiological and pathological conditions[3]. Therefore, mitochondrial AKAPs might represent novel therapeutic molecular targets for CVD.

Mounting evidence suggests that mitochondrial dysfunction and oxidative stress play a role in changes in gut barrier function and gut microbiota composition[4–6]. Recent studies have shown that several interactions exist between intestinal microbiota and the cardiovascular system, mediated by numerous and various mechanisms[6]. On the one hand, the gut microbiota and the related metabolites produced can modulate the function and survival of cardiomyocytes and other cardiac cell populations, under physiological or pathological conditions[7]. On the other hand, numerous studies demonstrate that the hemodynamic changes resulting from CVD can induce profound abnormalities of gut permeability and gut microbiota composition[5]. This evidence suggests the existence of a crosstalk between gut and the heart, even if the mechanisms and mediators remain unclear.

During my Ph.D. fellowship, I participated in several studies which contributed to increase the knowledge in this area of research.

Outline of the thesis

The thesis is divided into four parts:

Part I. **Transverse aortic constriction induces gut barrier alterations, microbiota remodeling and systemic inflammation.**

In this part of thesis, I report the results of the role of the intestine-heart axis in the murine modelof transverse aortic constriction.

Part II. **Mitochondrial a Kinase Anchor Proteins in Cardiovascular Health and Disease.**

In this second part of thesis, I collected my studies on the role the mitochondrial AKAPs in CVD.

Part III. **Partial loss of *Akap1* gene promotes cardiac dysfunction, gut barrier abnormalities, and alteration of gut microbiota composition during ageing.**

This section of the thesis is a collection of results aimed at investigating the role of *Akap*1 in cardiac dysfunction, gut barrier function and alterations of gut microbiota composition during aging.

Part IV. **Discussion and Conclusions.**

The last section of the thesis is a broad discussion of the addressed topics with the conclusions.

Part I

Transverse aortic constriction induces gut barrier alterations, microbiota remodeling and systemic inflammation.

Chapter 1

Background and study design

Several pathological conditions, including heart failure (HF), have been associated with gut barrier dysfunction and intestinal dysbiosis, with still largely undefined mechanisms[6,8]. Decreased cardiac output and peripheral vasoconstriction induced by HF, can promote intestinal hypoperfusion with consequent leaky gut. This condition promotes systemic inflammation and might affect gut microbiota composition[9,10].

A now large body of evidence suggest the potential roles of specific bacteria in the pathogenesis of cardiometabolic disorders and their therapeutic implications[11,12]. In addition, gut microbiota-derived molecules, either structural components or bioactive products, can exert remote effects through the activation of different signaling pathways in CVD[7,13,14]. In this context, despite species-specific limitations, experimental systems including animal models are crucial to test for causal connections and provide novel insight into host–microbiota interactions modeling human health and diseases.

The murine model of transverse aortic constriction (TAC) is one of the most well-established and widely used preclinical models of pressure overload-induced cardiac hypertrophy and failure[15].

In this study, we have evaluated gut microbiota composition, intestinal barrier integrity, intestinal and serum cytokines and serum endotoxin levels in C57BL/6 mice undergoing pressure overload by TAC for 1 and 4 weeks (1w, 4w). Mice subjected to left thoracotomy without aortic constriction (sham) for the same duration of time were used as control groups.

Chapter 2

Effects of transverse aortic constriction on gut permeability and systemic inflammation

As to be expected, mice subjected to Transverse Aortic Constriction (TAC) surgery show cardiac hypertrophy and systolic dysfunction. Immediately after TAC, abdominal aortic blood flow was significantly reduced in TAC mice compared to sham, resulting in intestinal hypoperfusion (Fig. 1A). Decreased intestinal perfusion in TAC 1w mice was associated to alterations of intestinal barrierintegrity, as shown by reduced mRNA expression of occludin (*Ocln*) and tight junction protein zonula occludens-1 (*Tjp1*) (Fig. 1 B, C), and reduced immunostaining of zonula occludens-1 (ZO- 1) after 1 week of pressure overload (Fig. 1D).

To determine the effects of TAC on gut barrier function, we analyzed circulating levels of Fluorescein Isothiocyanate-Dextran D4000 (FITC-dextran) at different time intervals after oral administration by gavage in sham 1w and TAC 1w mice. In TAC 1w mice, circulating levels of FITC-dextran significantly increased 1 h after oral gavage, and thereafter decreased. In contrast, time-course of FITC-dextran circulating levels was delayed in sham 1w mice compared to TAC 1w, reaching peak concentration 2 h after oral administration, and decreasing thereafter (Fig. 1E). Gut barrier function was still functionally impaired in TAC 4w mice, as shown by differences in circulating levels of FITC-dextran between TAC 4w and sham 4w mice 1 h after gavage (Fig. 1F). Colon expression levels of anti-inflammatory cytokine interleukin-10 (IL-10) were significantly reduced in TAC 1 w and TAC 4w colon samples compared to respective sham(Fig. 2A;). These changes were associated to the histological evidence of remarkable inflammatory infiltrate in murine colon samples from TAC 1w mice (Fig. 2B). Consistent with these results, serum levels of lipopolysaccharide (LPS) and proinflammatory cytokines tumor necrosis factor-α (TNF-α) and interleukin-1 (IL-1), were rapidly and persistently enhanced afterTAC surgery (Fig. 2C), while circulating levels of IL-10 were reduced in TAC mice (Fig. 2C– F).
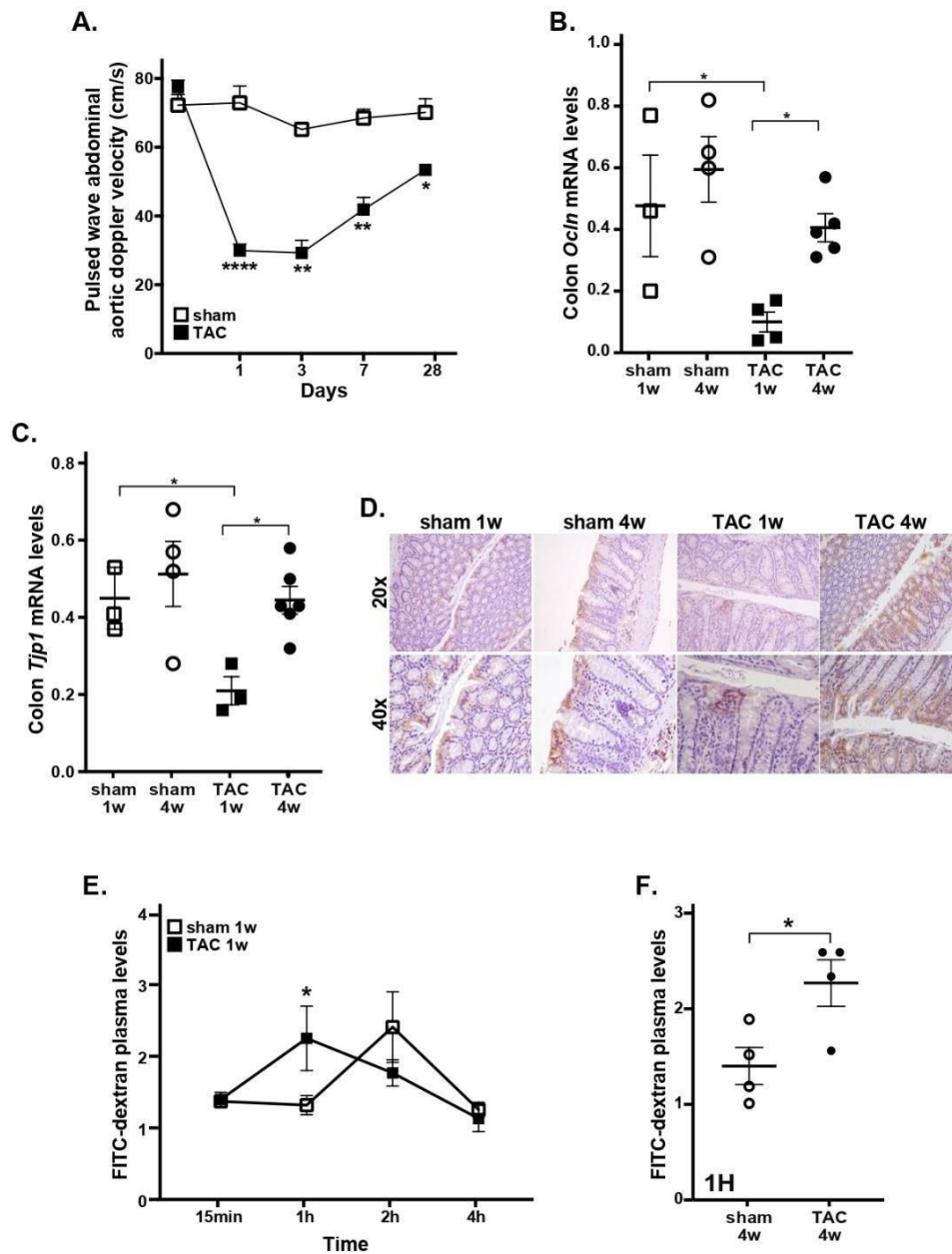
Figure 1. Effects of TAC or sham surgery on intestinal barrier integrity.

(A) Abdominal aortic blood flow (cm/s) was evaluated at 1, 3, 7 and 28 days after surgical procedure in sham and TAC mice by Pulsed Wave Doppler (sham n = 6; TAC n = 10). (B, C) mRNA expression levels of occludin (Ocln, B) and tight junction protein ZO-1 (Tjp1, C) in colon samples from sham or TAC mice (sham: n = 3–4; TAC: n = 3–6). (D) Representative images of immunohistochemical analysis of tight junction protein ZO-1 in colon samples from the different groups of mice (sham 1w: n = 6; sham 4w: n = 5; TAC 1w: n = 4; TAC 4w: n = 6). ZO-1 positive cells were stained in brown; bigger brown and deeper color represent higher ZO-1 protein levels. Pictures are shown at 20 × and 40 × magnification. (E) Plasma levels of FITC-dextran 4000 at

15 min, 1, 2, 4 h after gavage in sham 1w and TAC 1w mice (sham 1w: n = 14; TAC 1w: n = 12). (F) Plasma levels of FITC-dextran 4000 1 h after gavage in sham 4w and TAC 4w (sham 4w: n = 4; TAC 4w: n = 4). Results are presented as mean ± SEM. Statistical significances were assessed using one-way ANOVA followed by Newman-Keuls multiple comparison post-hoc test (A) or Tukey's comparison test as appropriate (B–F).

Figure 2
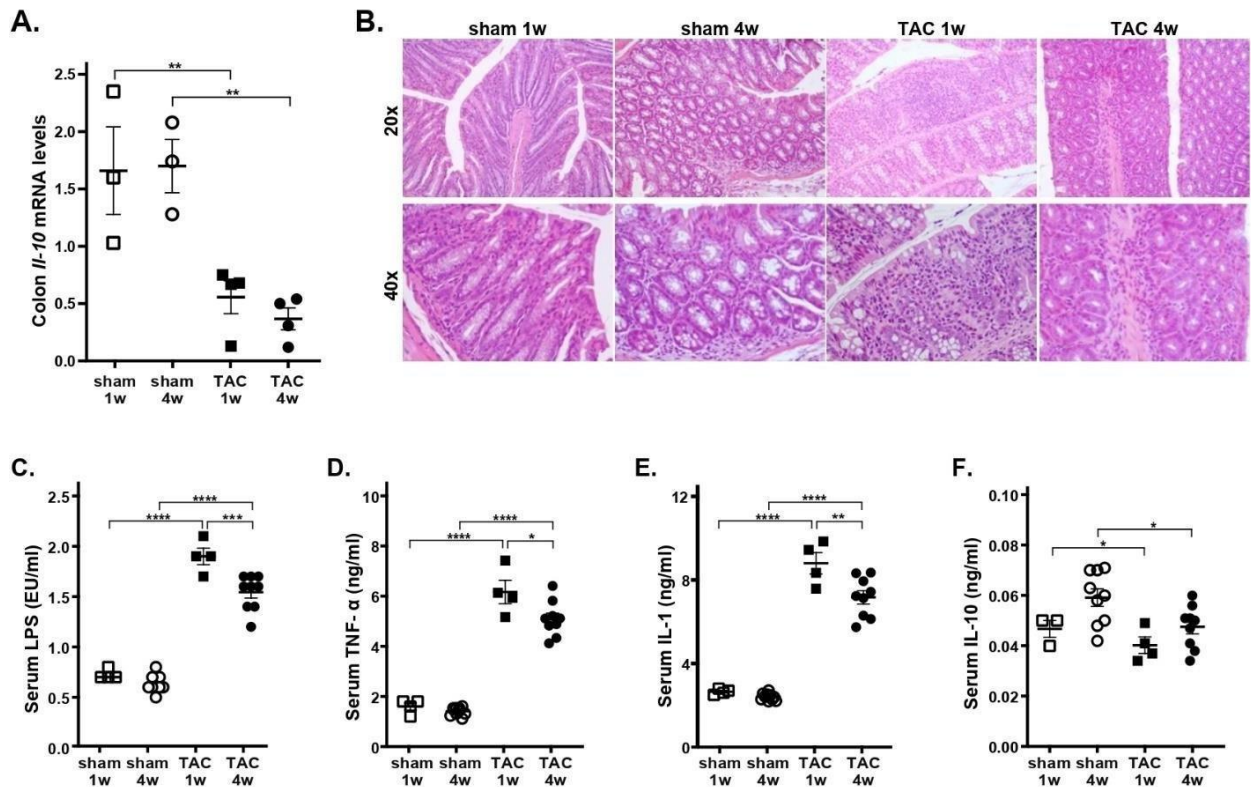
Figure 2. Effects of TAC or sham surgery on inflammation.

(A) mRNA expression levels of Interleukin-10 (Il10) in colon samples (sham: n = 3–4; TAC: n = 3– 6). (B) Representative hematoxylin and eosin–stained sections from colon tissues of mice at original magnifications ×20 and ×40. Histological evaluation of inflammatory cells infiltration was scored along the entire colon length, inspecting the colon mucosa, submucosa and transmural areas considering the following parameters: (a) severity of inflammatory cell infiltration (sham 1w = 0.83 ± 0.16, sham 4w = 1.40 ± 0.24, TAC 1w = 2.25 ± 0.25, TAC 4w = 1.83 ± 0.31); (b) extent of the inflammation as expansion of leukocyte infiltration (sham 1w = 1.17 ± 0.31, sham 4w = 1.20 ± 20, TAC 1w = 2 ± 0, TAC 4w = 1.50 ± 0.22); and (c) presence of fibrosis (sham 1w = 0 ± 0, sham 4w = 0 ± 0, TAC 1w = 0.25 ± 0.25, TAC 4w = 0.33 ± 0.21). Data reported are mean ± SEM (sham 1w: n = 6; sham 4w: n = 5; TAC 1w:

n = 4; TAC 4w: n = 6). Serum levels of (C)lipopolysaccharide (LPS), (D) tumor necrosis factor-α (TNF-α), (E) interleukin-1 (IL-1) and (F) IL-10 in all experimental groups (sham: n = 4–8; TAC: n = 4–9). Results are presented as mean ± SEM. Statistical significances were assessed using one-way ANOVA followed by Newman– Keuls multiple comparison post-hoc test (A) or Tukey's comparison test as appropriate (B–F).

Chapter 3

Pressure overload impact on gut microbiota composition

Gut barrier integrity is closely linked to gut microbiota composition, and they can be reciprocally affected, especially in response to external pathological causes. Differences in fecal microbiota composition among sham and TAC mice were determined by 16S rDNA sequencing and a good's coverage index > 99% was obtained at the rarefaction point of 26,396 reads/sample. Comparison of fecal gut microbiota communities among groups revealed significant changes of bacterial genera inside *Actinobacteria*, *Firmicutes*, *Proteobacteria* and TM7 *phyla*. Specifically, intergroup differences at genus and species levels were analyzed by the linear discriminant analysis (LDA) effect size (LEfSe), identifying the genera *Bifidobacterium*, *Lactobacillus*, *Turicibacter*, unclassified genus (u.g.) of RF32 and u.g. of F16 as characteristic of TAC mice, whereas the genus *Oscillospira* was significantly less abundant in TAC mice compared to sham at specific time windows (Fig. 3A). SPINGO high-resolution approach was used to obtain bacterial species assignment of key genera with significant differences among groups (Fig. 3B). After TAC, a significant increase in OTUs resembling *Bifidobacterium pseudolongum*, Turicibacter sanguinis, *Lactobacillus frumenti*, and an unclassified species belonging to *Proteobacteria phylum* (order RF32) was detected, along with decrease of species within *Oscillospira* genus (*Pseudoflavonifractor capillosus* and *Flavonifractor plautii*, Fig. 3B).

To predict functional effects of gut microbiota alterations induced by TAC, we performed a Phylogenetic Investigation of Communities by Reconstruction of Unobserved States (PICRUST) analysis. This analysis revealed a significant increase in pathways inducing L-lactate dehydrogenase after 1w TAC (pre-surgery: $2,445.6 \pm 272.9$; sham 1w: $2,038.4 \pm 323.9$; TAC 1w: $3,074 \pm 331.6$; $p < 0.05$ for sham 1w vs. TAC 1w according to two-tailed nonparametric Kruskal–Wallis test). Collectively, these data indicate that a significant remodeling of specific bacterial species abundance within identified key genera occurs soon after TAC, identifying a clear effect of the surgery on microbiota profiles and, possibly, on microbiota functionality.
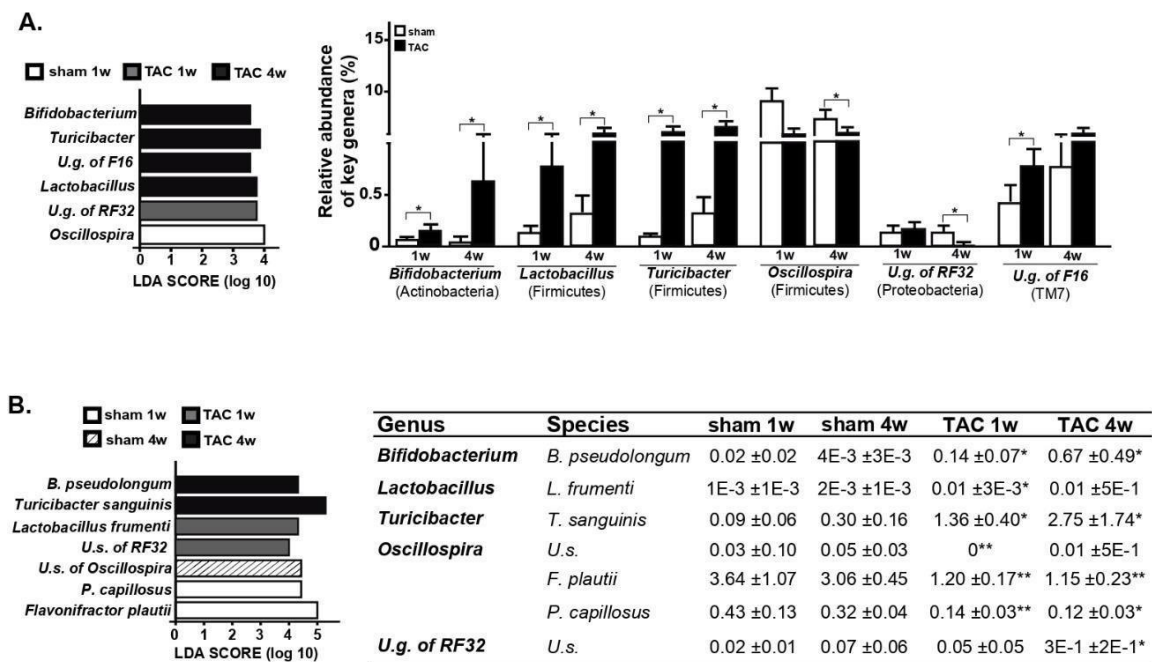
Figure 3. Gut microbiota composition after sham or TAC surgery in mice.

Gut microbiota differences based on 16S rDNA sequencing at genus (A) and species (B) taxonomic levels were identified using linear discriminant analysis (LDA) combined with effect size (LEfSe) algorithm. In each panel, LDA scores (left) and relative abundance (right) of key phylotypes discriminating sham and TAC bacterial communities are reported (sham n = 8; TAC n = 9). Statistical significances were assessed using LEfSe analysis with alpha values of 0.05 for both Kruskal–Wallis and pairwise Wilcoxon tests and a cutoff value of LDA score (log10) above 2.0 (*p < 0.05 and **p < 0.01 vs. correspondent sham).

Part II

Mitochondrial a Kinase Anchor Proteins in Cardiovascular Health and Disease.

Chapter 1
Mitochondrial AKAPs

The main source of cellular energy is produced by the mitochondria, moreover, their function consists in regulation cell survival, metabolism, calcium homeostasis and the production of ROS. Mitochondrial dynamics, the regulated balance of fusion and fission, represents a key aspect of mitochondrial function and is implicated in pathological conditions, including cardiovascular disorders such as cardiac hypertrophy, cardiac arrhythmias and HF[16,17].

The β1-adrenergic receptors (β1ARs) are members of the superfamily of heptahelical transmembrane receptors (7TMR), also known as G-protein-coupled receptors (GPCRs), and crucial regulators of multiple cardiovascular functions[18–20]. β1AR ligand binding induces receptor conformational changes that lead to the activation of G proteins and G-protein-mediated signaling, as well as G-protein-independent downstream effectors[21,22]. Stimulation of Gs by β1ARs increases intracellular levels of cAMP.

cAMP rise induced by different agonists can produce different physiological responses, even within the same tissue, depending on the spatial and temporal regulation of the cAMP gradient by adenylyl cyclases (AC), phosphodiesterases (PDEs) and the local activation of effectors, mainly represented by the "classical" cAMP-dependent PKA, cyclic nucleotide-gated ion channels and the more recently discovered exchange protein directly activated by cAMP (Epac)[23–25].PKA holoenzyme is composed of two regulatory (R) and two catalytic (C) subunits, anchored to membranes and discrete cellular locations by a large family of mitochondrial AKAPs that play a crucial role in the propagation of cAMP/PKA signals. By binding PKA regulatory subunits (R) and specific intracellular organelles, AKAPs act as scaffolds that integrate and direct signaling events to downstream targets to achieve efficient spatial and temporal control of their phosphorylation state[26–28] While the majority of AKAPs selectively bind PKA type II regulatory subunits (RII), dual- specificity AKAPs (D-AKAPs) bind to type I regulatory subunits (RI) and RII, potentially engaging distinct cAMP-responsive holoenzymes to specific intracellular locations. According to the cell type and pathophysiological context, the modulation of local signaling by AKAPs, either enhancement or disruption, transient or permanent, may regulate cardiovascular physiology, and its derangement may lead to pathological conditions.

cAMP/PKA pathway has been previously found to regulate several mitochondrial functions, such as respiration, mitochondrial dynamics, ROS production and apoptosis[29]. cAMP signals are carried to mitochondria by several AKAPs, including D-AKAP1 (encoded by the *Akap1*

gene), D-AKAP2 (*Akap10* gene), PAP7 (*Acbd3* gene), OPA1 (*Opa1* gene), WAVE-1 (*Wasf* gene), RAB32 (*Rab32* gene) and SKIP (SPHKAP gene), summarized in Table 1 and schematically illustrated in Figure 4[30–32]. Recent biochemical and immunocytochemical studies indicate that D-AKAP1 and D-AKAP2 are the predominant mitochondrial AKAPs exposed to the cytosolic compartment in ventricular myocytes; thereby, both RI and RII PKA subunits are associated with mitochondria[31,33,34]. The role of D-AKAP1 in CVD, it has been discussed in the next chapters.
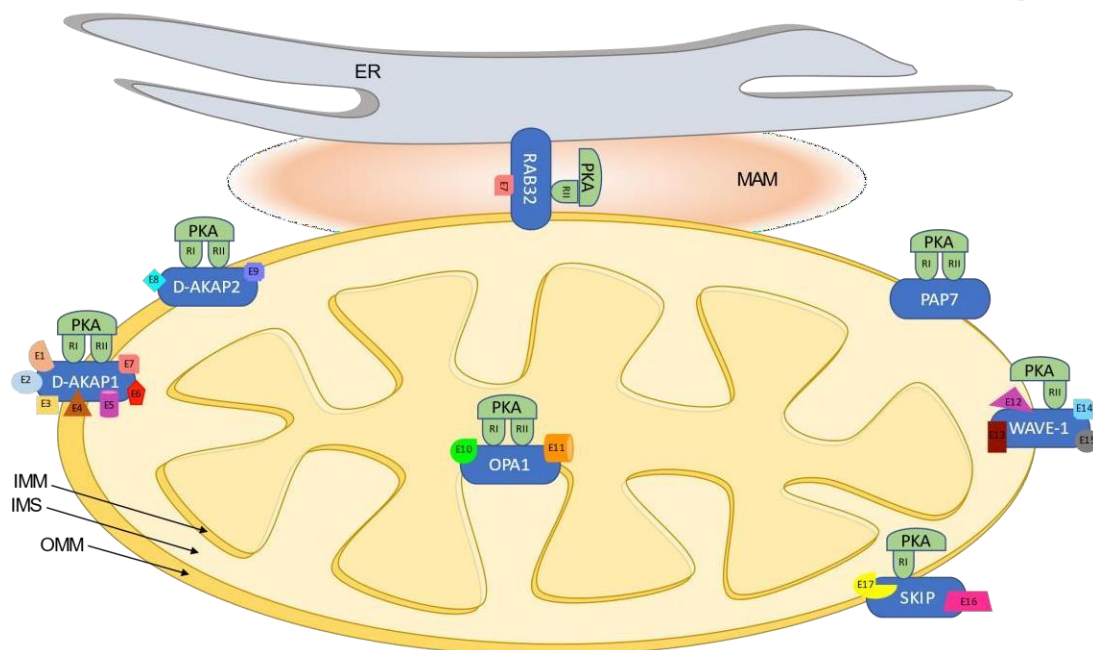
Figure 4. Mitochondrial AKAPs localization. *Schematic representation of mitochondrial AKAPs localization. Abbreviations used: endoplasmic reticulum, ER; intermembrane space, IMS; outer mitochondrial membrane, OMM; inner mitochondrial membrane, IMM; mitochondria-associated membranes, MAM; different binding effectors partners, E; Ras-related protein, RAB32; peripheral-type benzodiazepine receptor and cAMP-dependent protein-kinase-associated protein 7, PAP7; Wiskott Aldrich syndrome proteins, Wave-1; Sphingosine kinase type 1-interacting protein, SKIP; Optic atrophy 1, OPA1; dual- specificity A-kinase anchoring protein, D-AKAP1, D-AKAP2.*

Table 1. Mitochondrial AKAPs and their known cardiovascular functions

Gene	Protein	Effector of AKAP	Interaction with PKA subunits	Mitochondrial localization	Mitochondrial effects	Cardiovascular functions
Akap1	D-AKAP1	PP1(E1), Src(E2), PDE4(E3),Calcineurin(E4), AGO2(E5), NCX3(E6), DRP1(E7)	RI, RII	OMM	Apoptosis, mitochondrial fusion, mitochondrial respiration	Modulates infarct size after coronary artery ligation and post-ischemic cardiac remodelling, cardiac hypertrophy and pressure overload-induced cardiac dysfunction, endothelial function and angiogenesis
Akap10	D-AKAP 2	Rab 4(E8), Rab11(E9)	RI, RII	OMM	Mitochondrial dynamics, ROS production and apoptosis	Modulate cardiovascular integrity barrier and controller of pacemaker cells sensitivity to cholinergic stimulation
Acbd3	PAP7		RI, RII	OMM	Cholesterol transport	Unknown
Opa1	OPA1	OMA1(E10), YME1L(E11)	RI, RII	IMM	Mitochondrial fusion and fission, stabilizing mitochondrial cristae, increasing mitochondrial respiratory efficiency	Modulates cardiac function and hypertrophy, metabolic shift of increased glucose uptake
Wasf	WAVE-1	BAD(E12), Pancortin2(E13),GK(E14), BCL-XL(E15)	RII	OMM	Mitochondrial trafficking	Unknown
Rab32	RAB32	DRP1(E7)	RII	MAM	Endoplasmic reticulum Ca^{2+} handling, mitochondrial fusion, apoptosis	Unknown
Sphkap	SKIP	ChChdl3(E16), S1P(E17)	RI	OMM	Mitophagy	Modulates infarct size, apoptosis and cytochrome c release after myocardial ischemia-reperfusion injury

Abbreviations: PKA, protein kinase A; RI, regulatory subunit type I; RII, regulatory subunit type II; OMM, outer mitochondrial membrane; IMM, inner mitochondrial membrane; MAM, mitochondria-associated membrane.

Chapter 2

D-AKAP1 in cardiovascular system and metabolism

D-AKAP1 is a mitochondrial AKAP encoded by the *Akap1* gene and expressed in various organs and cell types, including the cardiovascular system, and it is highly expressed in the human heart[31,35,36]. AKAP149 and the smaller variant s-AKAP84 are prototypic members of the D-AKAP1 family, sharing a similar 525-aminoacid NH2-terminal core but diverging significantly at the C-terminus. PKA binding domains of the rat, mouse and human D-AKAP1 homologues are highly conserved and bind PKA RII subunits with high affinity and RI with lower affinity. The first 30 NH2-terminal residues mediate the targeting of D-AKAP1-PKA complexes to the outer mitochondrial membrane (OMM, Fig. 4). Within this motif, AKAP149 and S-AKAP84 present a conserved tubulin-binding motif, allowing interaction with both tubulinpolymers and soluble microtubules[37]. Although D-AKAP1 has been primarily localized at the OMM, some variants have also been localized intracellularly at other intracellular locations, including the nuclear membrane and the endoplasmic reticulum. In addition to transcriptional regulation, D-AKAP1 undergoes rapid ubiquitination and proteasomal degradation upon hypoxia, mediated by the E3 ubiquitin ligase seven in-absentia homologue (Siah2)[38]. Since D- AKAP1 controls mitochondria dynamics through PKA-dependent inhibitory phosphorylation of Dynamin-related protein 1 (Drp1) and PKA-independent inhibition of Drp1– Mitochondrial fission 1 protein (Fis1) interaction, its reduced availability mediated by Siah2 relieves Drp1 inhibition, increasing its interaction with Fis1, thus resulting in mitochondrial fission[39]. A multivalent signaling complex nucleated by D-AKAP1 on the OMM that includes, among other molecules, PKA, tyrosine-protein kinase Src, serine/threonine protein phosphatase 1 (PP1), cyclic nucleotide phosphodiesterase 4 (PDE4), Drp1, calcineurin, Na^+/Ca^{2+} exchanger NCX3 and argonaute 2 protein (Ago2), has been previously identified as an essential regulator of multiple mitochondrial functions[36,40,41]. Several studies demonstrate that both in cardiomyocytes and in several murine models of cardiovascular disease, D-AKAP1 deficiency impairs mitochondrial structure and respiratory function, reduces ATP production and increases cardiomyocyte apoptosis via enhanced mitochondrial ROS production[42–44]. Moreover, D- AKAP1 expression is reduced in hearts of streptozotocin-induced diabetic mouse models, and its genetic inactivation significantly enhances cardiac dysfunction in diabetic mice. D-AKAP1 has a role in blood pressure regulation, in fact, it was demonstrated that compared to wild type (*wt*), *Akap1*$^{-/-}$ mice of either sex display a mild but significant increase in systolic blood pressurelevels even if within the normal range, while *Akap1*$^{+/-}$ mice display an intermediate phenotype.

These differences can be largely attributed to a selective impairment in endothelium-dependent vasorelaxation in mice with partial or total loss of D-AKAP1[44]. Indeed, D-AKAP1 inactivation also profoundly alters mitochondrial structure and function of vascular endothelial and smooth muscle cells, reducing mitochondrial membrane potential, increasing mitochondrial ROS production and, finally, enhancing hypoxia-induced cell dysfunction or death [42,43]. In particular, $Akap1^{-/-}$ endothelial cells display remarkable mitochondrial alterations impacting multiple *in vitro* and *in vivo* functions, such as proliferation, migration and differentiation [44].

Chapter 3

D-AKAP1 in myocardial ischemia and cardiac hypertrophy

In myocardial ischemia, D-AKAP1 plays a protective role, regulating mitochondrial structure and function, ROS production and cell survival. It was demonstrated that upon *in vitro* hypoxia, cells lacking Siah2 display higher D-AKAP1 levels, and this is associated with reduced fission and apoptosis[39]. Moreover, after coronary artery ligation to induce myocardial infarction (MI), *Akap1*$^{-/-}$ mice display remarkable abnormalities in mitochondrial structure, increased cardiomyocyte death and infarct size, aggravating cardiac[45] remodeling and accelerating HF development. Genetic inactivation of *Siah2* prevents D-AKAP1 degradation after MI, reducing infarct size and ameliorating cardiac remodeling and survival[43].

Cardiac hypertrophy is the first general response of the heart to physiological or pathological loads. It was shown that pathological stress is able to specifically activate detrimental signaling pathways in the heart[15]. Among these, abnormalities in βAR signaling are the best studied and characterized, seem to be mechanistically linked to the development of cardiac dysfunction and are hallmarks of the failing human heart[46]. In response to pressure overload, cAMP response element-binding protein (CREB) phosphorylation is rapidly and significantly inhibited, altering PKA-dependent transcription of CREB-induced genes, including D-AKAP1. Thus, D-AKAP1 down-regulation may be a direct consequence of this block since its transcription is dependent by cAMP. In addition, more recent data indicate that D-AKAP1 is also subjected to ubiquitin-dependent degradation[38], and this may be operating in the early phases of cardiac stress, such as acute myocardial ischemia.

D-AKAP1 downregulation is associated with marked abnormalities in mitochondrial morphology and structure at electron microscopy, reduced aconitase activity and increased mitochondrial ROS generation, suggesting that D-AKAP1 is an important regulator of mitochondrial function and ROS generation in the overloaded heart[45]. We and others have shown that after TAC, *Akap1*$^{-/-}$ mice display enhanced cardiomyocyte and left ventricle hypertrophy and accelerated progression towards heart failure (HF) compared to wild type mice. This phenotype is associated with a significant increase in cardiac apoptosis as well as a lack of activation of protein kinase B signaling after pressure overload [42]. Taken together, these results suggest that in vivo genetic ablation of D- AKAP1 promotes pathological cardiac hypertrophy and HF, indicating D-AKAP1 as a novel repressor of pathological left ventricular remodeling and failure.

Part III

Partial loss of AKAP1 promotes cardiac dysfunction, gut barrier abnormalities, and alteration of gut microbiota composition during ageing.

Chapter 1

Background and study design

As discussed in the previous chapter, mitochondrial AKAPs play a crucial role in mitochondrial structure and function, ROS production and cardiomyocyte survival. Recent studies have shown that there is a correlation between ROS production, gut permeability, and cardiomyocyte dysfunction[5]. Although it is known that oxidative stress underlies the processes of cellular senescence, the molecular mechanisms directly involved in cardiovascular aging are currently poorly understood. Furthermore, there is a correlation between aging, ROS production, intestinal permeability and gut microbiota composition[5,47]. In particular, profound functional and structural changes of the intestinal barrier and gut microbiota composition have been previously identified in patients suffering from HF[48,49], but whether the normalization of such dysfunction is able to improve the pathological cardiovascular phenotype is currently unknown. The aim of this study was to identify the role of AKAP1 in cardiovascular aging and highlight the complex interplay between cardiac dysfunction, gut barrier integrity, gut microbiota composition and aging in young (6-month-old, 6m) and old (24-month-old,

24m) *wild type* (*wt*) and *Akap1* heterozygous *knockout* mice (*Akap1*^{+/-}).
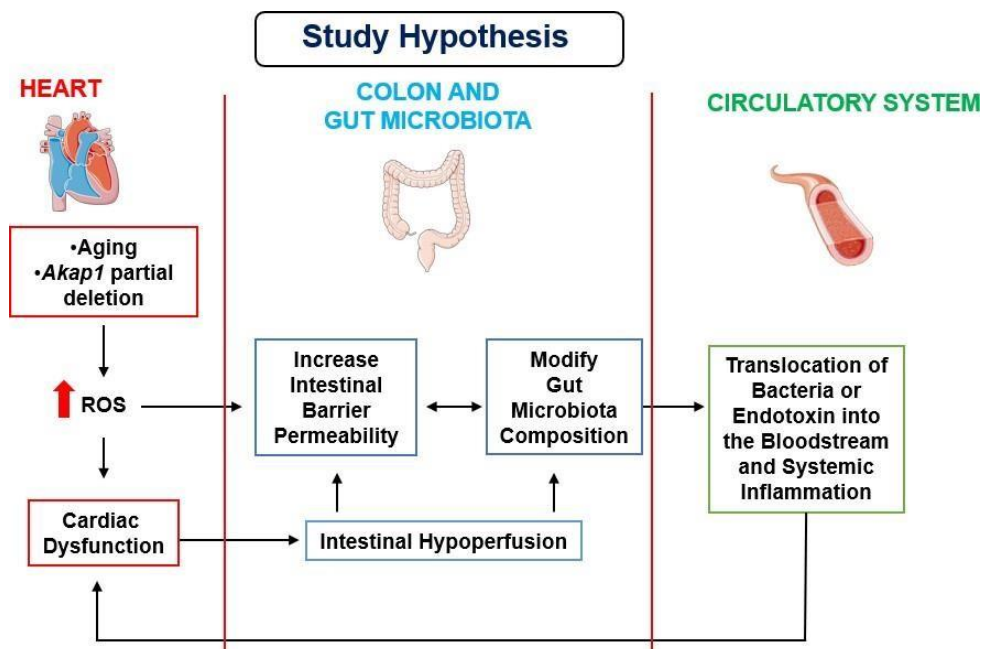

Figure 5: *Study Hypothesis*

Chapter 2

Partial loss of *Akap1* gene promotes cardiac dysfunction during aging.

We have previously demonstrated that myocardial levels of AKAP1 decrease in response to pressure overload[42], suggesting a role for this adaptor protein in the transmission of hypertrophic signals in the myocardium. However, the effects of heterozygous *Akap1* genetic deletion on cardiac remodeling in response to aging are currently unknown. Consistent with our previous results, AKAP1 cardiac levels were significantly decreased in 24m *Akap1*$^{+/+}$ mice compared to 6m *Akap1*$^{+/+}$ (Fig. 6A) demonstrating that downregulation occurs during aging. In comparison with the 24 m *Akap1*$^{+/+}$, 24m *Akap1*$^{+/-}$ mice demonstrated increased left-ventricular (LV) wall thickness, LV dilation, and systolic dysfunction (Fig. 6, B–F).

Specifically, in morphometric analysis, 24m *Akap1*$^{+/-}$ mice exhibited a significant increase in left ventricular weight (LVW) to body weight (BW) and heart weight (HW) to body weight (BW) ratios compared to their respective controls 6m and 24m *Akap1*$^{+/+}$ (Table 2 and Fig. 6B). Aging inevitably leads to impairment in LV systolic function, but partial deletion of *Akap1* gene exacerbates and anticipates this condition. As expected, 24m *Akap1*$^{+/-}$ mice shown a significant decrease of % Fractional Shortening (%FS) compared to 24m *Akap1*$^{+/+}$ (Fig. 6D). Reduction in %FS observed in 24m *Akap1*$^{+/-}$, resulted by increase in both LV end-diastolic diameter (LVEDd) and LV end-systolic diameter (LVESd) (Fig. 6E, F).

Cardiac histology revealed a significant increase in cardiomyocyte cross-sectional area and increase fibrotic area in 24m *Akap1*$^{+/-}$ hearts compared to 24m *Akap1*$^{+/+}$ (Fig. 6, C and H). Moreover, as marker of HF, we tested B-type natriuretic peptide (BNP) mRNA expression levels in the myocardium of different group mice. Consistent with previous results, BNP levels were significantly increased in 24m *Akap1*$^{+/-}$ hearts compared to 24m *Akap1*$^{+/+}$ mice (Fig. 6G).
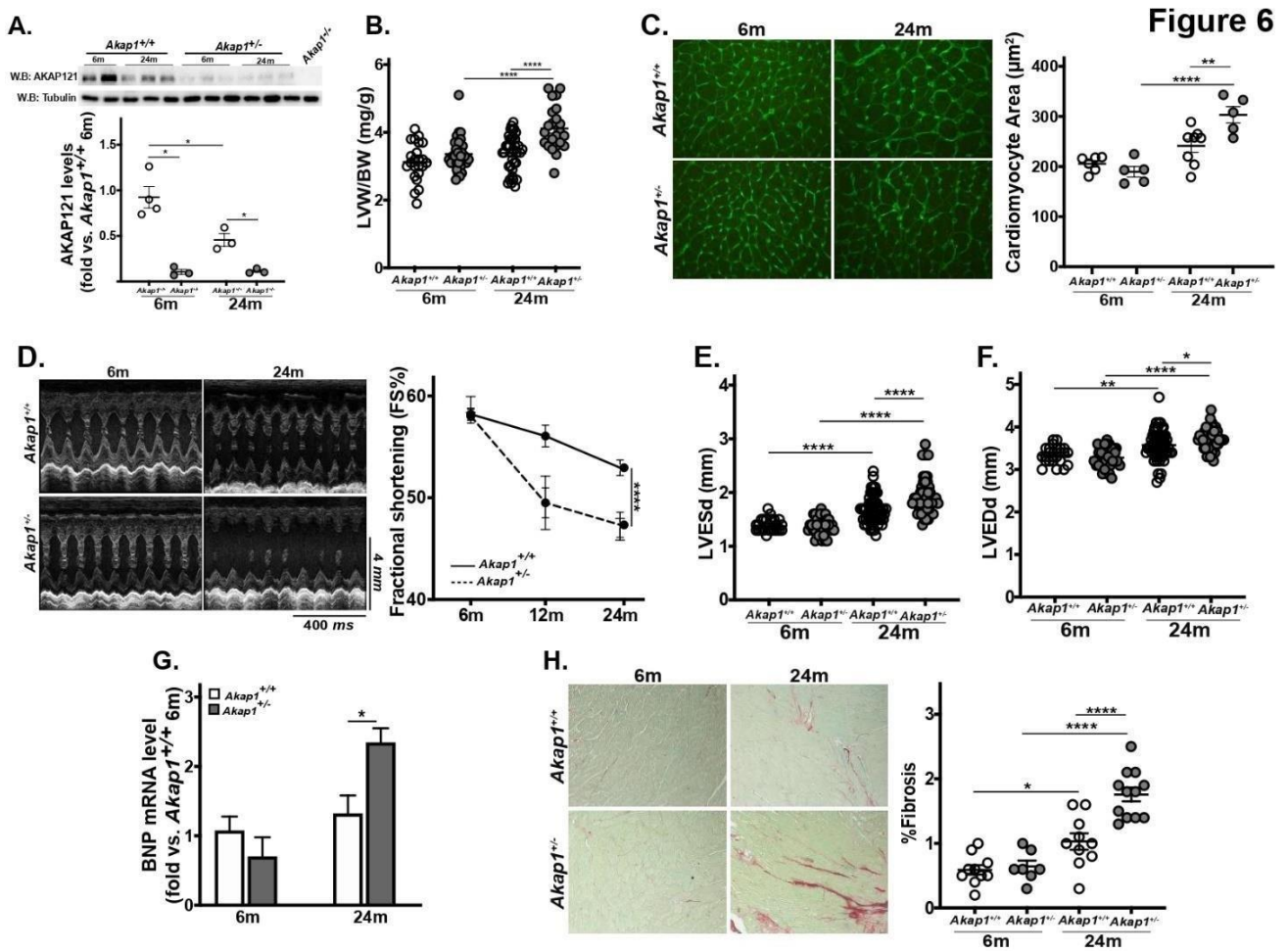
Figure 6: Partial deletion of *Akap1* gene promote HF during aging.

(A) Representative immunoblot (left) and densitometric analysis (right) of protein levels in hearts from 6m and 24m Akap1^{+/+}, Akap1^{+/-} mice. Tubulin was used as control of loading sample. (B) Graphs showing cumulative data of left ventricular weight (LVW) to body weight (BW) 6m and 24m Akap1^{+/+}, Akap1^{+/-} mice. (C) (Left) Representative images of wheat germ agglutinin (WGA) staining of cardiac transversal sections from 6m and 24m Akap1^{+/+}, Akap1^{+/-} mice (DAPI was used as nuclei counterstaining. Scale bar: 20 μm. (Right) graphs showing cumulative data of multiple independent experiments analyzing cardiomyocytes cross-sectional area. (D) (Left) Representative left ventricular (LV) M-mode echocardiographic tracings from 6m and 24m Akap1^{+/+}, Akap1^{+/-} mice. (Right) Cumulative data of % fractional shortening, left ventricular end- systolic diameter (LVESd; E) and left ventricular end-diastolic diameter (LVEDd; F) in 6m and 24m Akap1^{+/+}, Akap1^{+/-} mice. (G) mRNA levels of BNP in cardiac samples from 6m and 24m Akap1^{+/+}, Akap1^{+/-} mice. (H) Representative images of Picrosirius red staining of cardiac transversal sections from 6m and 24m Akap1^{+/+}, Akap1^{+/-} mice. Scale bar: 40 μm. (Right) graphs showing cumulative data of multiple independent experiments

analyzing percentage of fibrosis. (*p<0.05 vs. 6m Akap1^+/+ or 24m Akap1^+/+). Results are presented as mean ± SEM. Statistical significance were assessed using multiple comparisons were made by two-way ANOVA with Tukey correction *p≤0.05, **p≤0.01, ***p≤0.001, ****≤0.0001).

Table 2. Cardiac morphometry and echocardiography of mice from the different groups

	6m *Akap1*^+/+ (n=22)	24m *Akap1*^+/+ (n=34)	6m *Akap1*^+/- (n=34)	24m *Akap1*^+/- (n=32)
Morphometry				
BW, g	27.5 ± 0.6	28.7 ± 0.3	26.6 ± 0.5	29.9 ± 0.4*
LVW, mg	83.8 ± 2.4	107.3 ± 3.7*	88.1 ± 2.4	119.3 ± 3.6*#
HW, mg	115.3 ± 3.2	143.9 ± 4.8*	116.8 ± 3.2	165.5 ± 4.8*#
LVW/BW, mg/g	3.1 ± 0.1	3.6 ±0.1*	3.3 ± 0.1	4.1 ± 0.1*#
HW/BW, mg/g	4.3 ± 0.1	4.9 ±0.1*	4.4 ± 0.1	5.5 ±0.2*#
Echocardiography	(n=41)	(n=73)	(n=42)	(n=55)
LVEDd, mm	3.3 ± 0.04	3.6 ± 0.04*	3.2 ± 0.04	3.7 ± 0.03*#
LVESd, mm	1.4 ± 0.02	1.7 ± 0.03*	1.4 ± 0.03	2.0 ± 0.05*#
IVSd, mm	0.8 ± 0.03	0.9 ± 0.01*	0.8 ± 0.02	0.9 ± 0.02*
PWd, mm	0.8 ±0.02	0.9 ± 0.01	0.8 ± 0.02	1.0 ± 0.02*
FS, %	58.2 ± 0.6	53.2 ± 0.7*	58.4 ± 0.7	47.3 ± 1.09*#
HR, bpm	595 ± 11.6	563 ± 8.8*	573 ± 13	604 ± 9.7*#

Abbreviations used: Body weight, **BW**; left ventricle weight, **LVW**; heart weight, **HW**; left ventricular end-diastolic diameter, **LVEDd**; left ventricular end-systolic diameter, **LVESd**; interventricular septum end-diastolic diameter, **IVSd**; posterior wall end-diastolic diameter, **PWd**; fractional shortening, **% FS**; heart rate, HR. Results are presented as mean ± SEM. Statistical significances were assessed using multiple comparisons were made by two-way ANOVA with Tukey correction p≤0.05 vs. correspondent 6m; # p≤0.05 vs. 24m *Akap1*^+/+.

Chapter 3

Heterozygous *Akap1* deletion modulates gut permeability, gut microbiota composition and systemic inflammation during aging.

Systemic inflammation and gut permeability were assessed in 6m and 24m *Akap1*$^{+/+}$ and *Akap1*$^{+/-}$ mice. Serum levels of LPS were significantly increased in 24m *Akap1*$^{+/-}$ mice compared to 24m *Akap1*$^{+/+}$ (Fig. 7A). Levels serum of pro-inflammatory cytokines IL-1 and IL-6, tumor TNF-α and LDH were significantly increased in 6m *Akap1*$^{+/-}$ mice, while levels of anti-inflammatory IL-10 were significantly decreased compared to 6m *Akap1*$^{+/+}$ (Fig. 7, B-F).In addition, IL-1, IL-6, TNF- α and LDH were significantly increased in 24m *Akap1*$^{+/-}$ mice, compared to 24m *Akap1*$^{+/+}$ (Fig. 7, B-E). To investigate *in vivo* intestinal permeability, we analyzed circulating levels of FITC-dextran D4000 after administration by oral gavage. Plasma level of FITC-dextran D4000, 15 minutes after oral gavage, were significantly increased in 6m and 24m *Akap1*$^{+/-}$ mice groups compared their respectively aged *Akap1*$^{+/+}$ mice (Fig. 7 J). In addition, colon mRNA expression of *Ocln* and *Tjp1* were decreased in aged 24m *Akap1*$^{+/-}$ mice compared to 24m *Akap1*$^{+/+}$ (Fig. 7, G-H). Colon expression levels of pro-inflammatory cytokine interleukin (IL-1b) were significantly increased in 24m *Akap1*$^{+/-}$ mice, compared to 24m *Akap1*$^{+/+}$ (Fig. 7I). This result show that 24m *Akap1*$^{+/-}$ mice exhibit increased systemic inflammation and leaky gut.

Figure 7
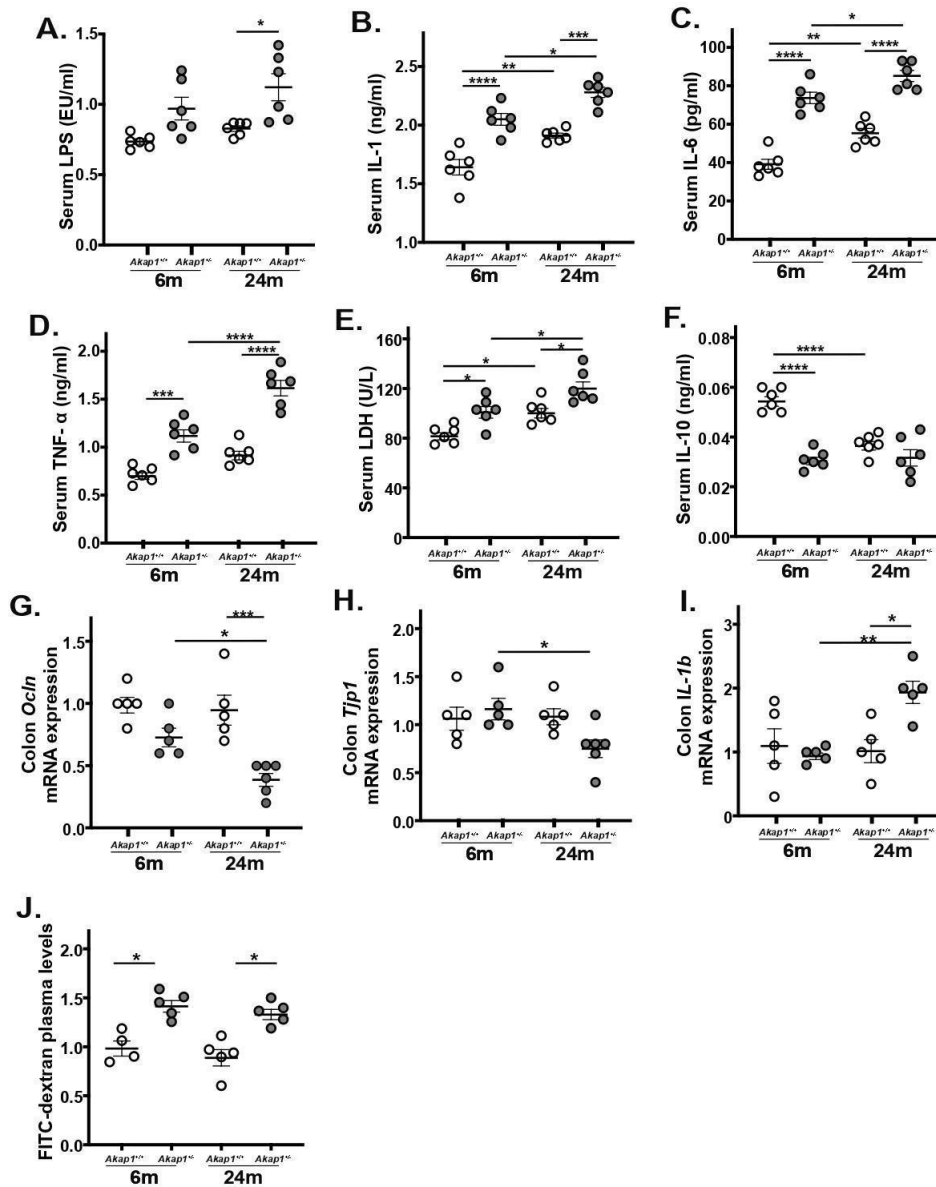
Figure 7: Partial deletion of *Akap1* gene promote systemic inflammation and gut permeability. *Serum levels of LPS (A), IL-1(B), IL6(C), TNF- α(D), LDH(E), IL10(F) in 6m and 24m Akap1$^{+/+}$, Akap1$^{+/-}$ mice. mRNA expression levels of, Ocln (G), Tjp1 (H) and IL-1(I) in colon samples from 6m and 24m Akap1$^{+/+}$, Akap1$^{+/-}$ mice. (J) Plasma levels of FITC-dextran 4000 15 minute after oral gavage in 6m and 24m Akap1$^{+/+}$, Akap1$^{+/-}$ mice. Results are presented as mean ± SEM. Statistical significances were assessed using multiple comparisons were made by two-way ANOVA with Tukey correction *p≤0.05, **p≤0.01, ***p≤0.001 ****≤0.0001).*

To identify the microbial signature of *Akap1*^{+/-} mice, we analyzed the differences in abundance of all 2,042 Operational Taxonomic unit (OTUs) between age-matched *Akap1*^{+/+} and *Akap1*^{+/-} and within the same genotype between 6m and 24 m aged mice. Differentially abundant OTUs were identified using LDA effect size analysis (LefSE; LDA score >2 and alpha <0.5). To identify the microbial signature of different groups, only differentially abundant OTUs with LDA score > 3 have been considered as key phylotypes. As shown in Figure 8, we identify a significant increase in 24m *Akap1*^{+/-} of the species *Ruminococcus Torques* and a significant reduction of *Blautia_producta*. Ruminococcus *Torques* and *Blautia_producta* are associated respectively to mucin degradation and butyrate production. These conditions of dysbiosis have been both identified in patients with CVD[50,51].
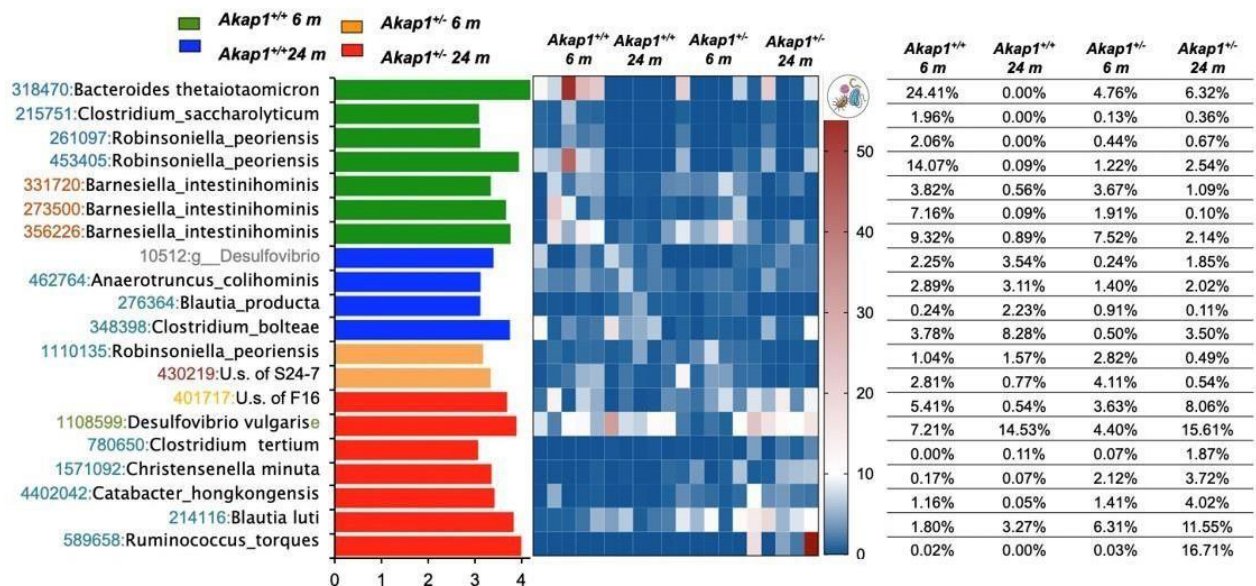
Figure 8: *Gut microbiota differences based on 16S rDNA sequencing at genus and species taxonomic levels were identified using linear discriminant analysis (LDA) combined with effect size (LEfSe) algorithm. In panel, LDA scores (left) and relative abundance (right) of key phylotypes discriminating Akap1*^{+/+} *and Akap1*^{+/-} *bacterial communities are reported.*

Chapter 4

Faecal microbiota transplantation (FMT) modulates cardiac function, gut barrier dysfunction and systemic inflammation.

To test whether gut microbiota composition together with gut permeability alteration and systemic inflammation can affect cardiac function, faecal microbiota transplantation (FMT) was performed for five weeks. Antibiotics treatment was conducted for 7 days in all mice groups except donors group, and the transplant procedure was performed starting on day 8 (1 day after the end of antibiotics treatment), three times per week for 5 consecutive weeks as previously described[52]. Fecal samples were collected for bacterial counts and 16S rDNA sequencing from all recipient and control mice at each time point (prior to antibiotic administration, immediately after the full antibiotic regimen, before the beginning of FMT, and 5 weeks after FMT).

In a first set of experiments (Fig. 9), fecal pellets from 24m $Akap1^{+/-}$ mice (24m $Akap1^{+/-}$ donors) were transplanted into recipient 6m $Akap1^{+/+}$ and 24m $Akap1^{+/+}$ mice (Group 1: 6m $Akap1^{+/+}$ FMT $^{(24m)}$; Group 2: 24m $Akap1^{+/+}$ FMT $^{(24m)}$). As control groups were used 6m and 24m $Akap1^{+/+}$ mice (Group 3: 6m $Akap1^{+/+}$ vehicle; Group 4: 24m $Akap1^{+/+}$ vehicle). The control groups received oral gavages of vehicle (phosphate-buffered saline).
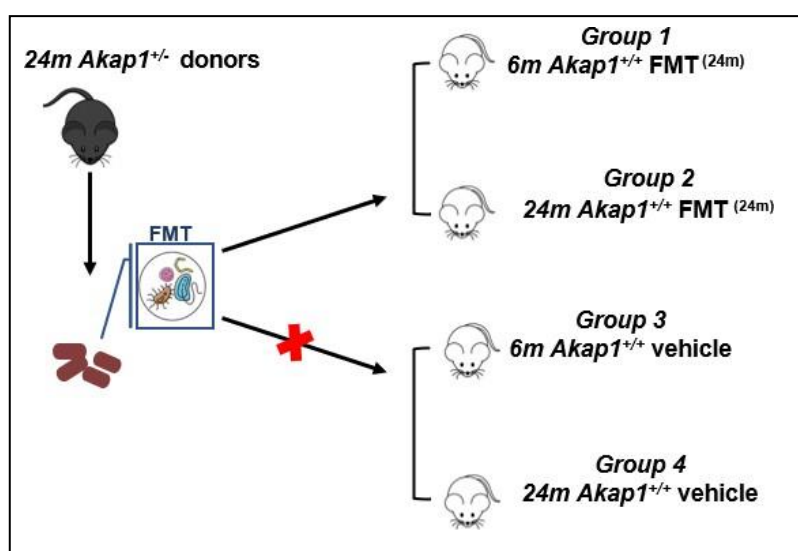
Figure 9: *Schematic representation of FMT using 24m Akap1$^{+/-}$ mice as feces donors.*

At the end of the experimental treatment, FMT had impact on cardiac function, specifically, %FS was significant reduced in mice of Groups 1 and 2 compared to their respective vehicle-treated controls (Groups 3 and 4), as shown in Fig.10A. Moreover, cardiac BNP levels were

significant LV increased in mice of Groups 1 and 2 compared to Groups 3 and 4 (Fig. 10B). Next, we evaluated the effect of gut microbiota transplantation in systemic inflammation. After 5 weeks of FMT treatment, serum levels of LPS, IL-1, IL-6 and TNF-α were significantly increased in mice of Groups 1 and 2 compared to Groups 3 and 4 (Fig. 10C-F). Moreover, gut permeability and colon inflammation were increased in mice of Groups 1 and 2 compared to Groups 3 and 4, as shown by reduced mRNA expression *Ocln* and *Tjp1* (Fig. 10G-H) and increased levels mRNA expression of TNF-α (Fig. 10I).
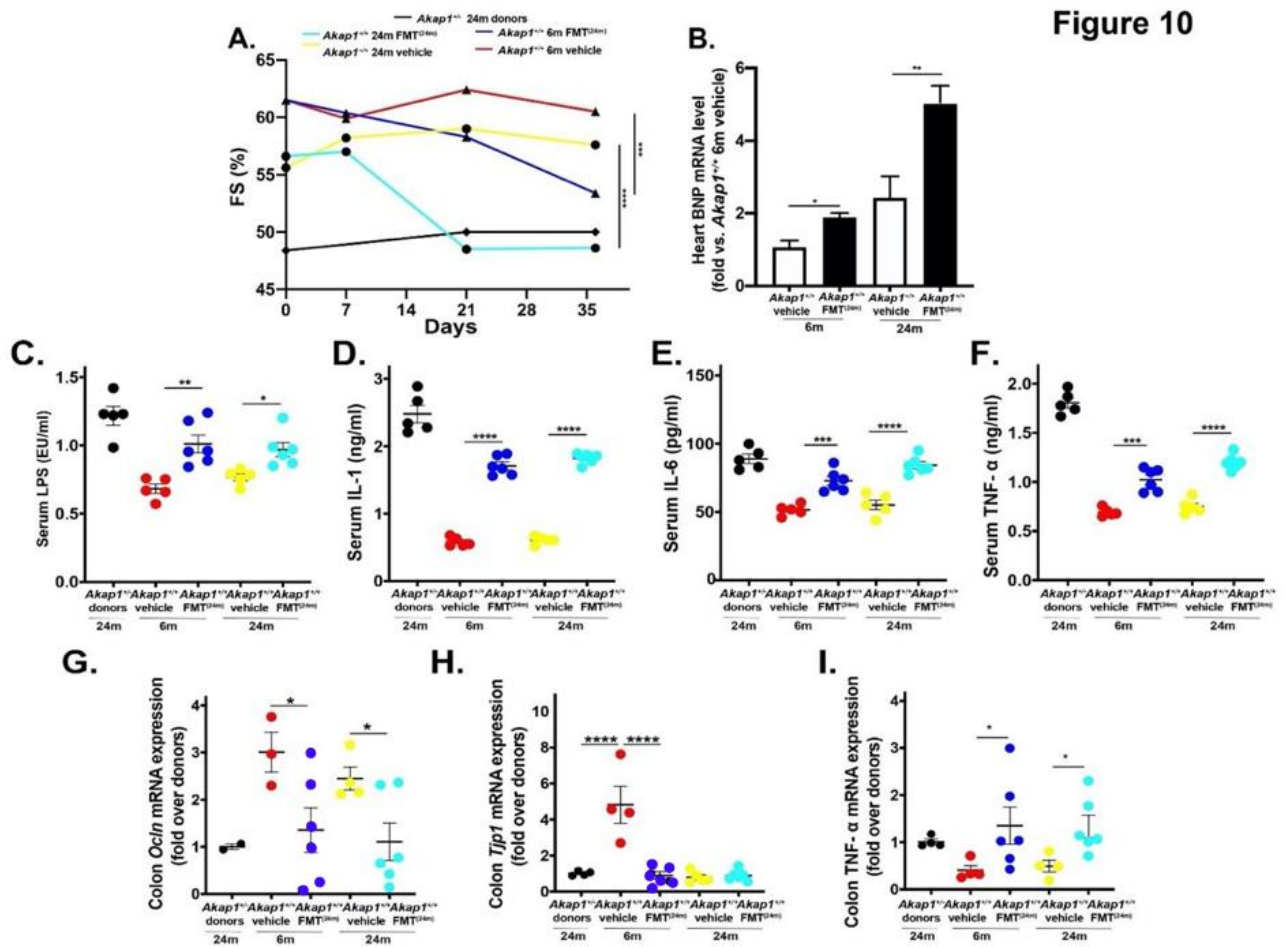
Figure 10: Unhealthy FMT modulates cardiac disfunction, leaky gut and systemic inflammation. *Cumulative data from 24m Akap1^{+/-} donors, 6m Akap1^{+/+} FMT (24m), 24m Akap1^{+/+} FMT (24m) and 6, 24 m Akap1^{+/+} vehicle of: % fractional shortening from(A); mRNA levels of BNP in cardiac samples (B); Serum levels of LPS (C), IL-1(D), IL6(E), TNF-α(F);mRNA expression levels of, Ocln (G), Tjp1 (H) and TNF- α (I). Results are presented as mean ± SEM. Statistical significances were assessed using multiple comparisons were made by two-way ANOVA with Tukey correction *p≤0.05, **p≤0.01, ***p≤0.001 ****≤0.0001).*

In a second set of experiments, fecal microbiota from 6m $Akap1^{+/+}$ mice (6m $Akap1^{+/+}$ donors) was transplanted in recipient 24m $Akap1^{+/-}$ mice (Group 5: 6m $Akap1^{+/-}$ FMT $^{(6m)}$). As control group was used 24m $Akap1^{+/-}$ (Group 6: 24m $Akap1^{+/-}$ vehicle).
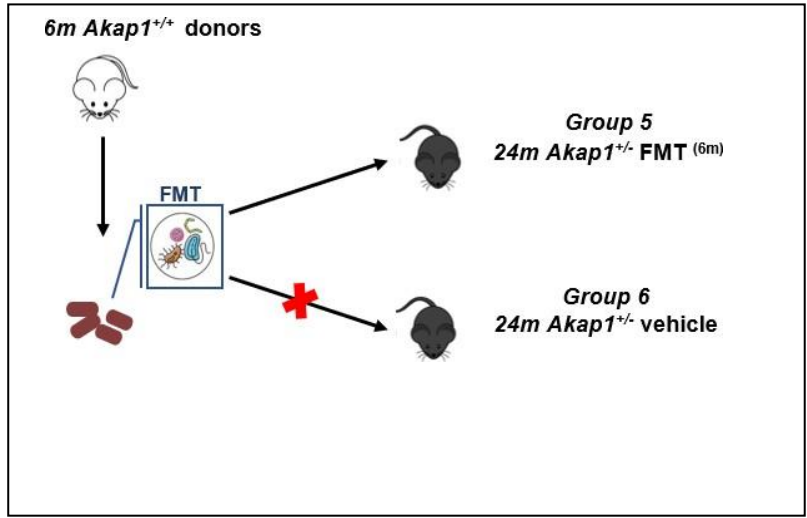
Figure 11: *Schematic representation of FMT using 6m Akap1$^{+/+}$ mice as feces donors.*

At the end of 5 weeks of FMT treatment, mice of Group 5 displayed a significant improvement of %FS (Fig. 11A) and a significant reduction of cardiac BNP levels (Fig. 11B) compared to Group 6. Similarly, serum levels of LPS, TNF-α and IL-1 were significantly decreased in mice of Group 5 compared to Group 6 (Fig. 11C-E), while levels of interleukin-10 (IL-10) were significantly increased in mice of Group 5 (Fig. 11F). No differences were found in IL-6 serum levels between the groups (Figure 11 G). Colon permeability was significantly improved after FMT using 6m $Akap1^{+/+}$ mice as feces donors, as shown by increased mRNA expression of *Ocln* in mice of Group 5 compared to Group 6 (Fig. 11H), while mRNA expression levels of *Tjp1* were not different between the groups Fig. 11I).
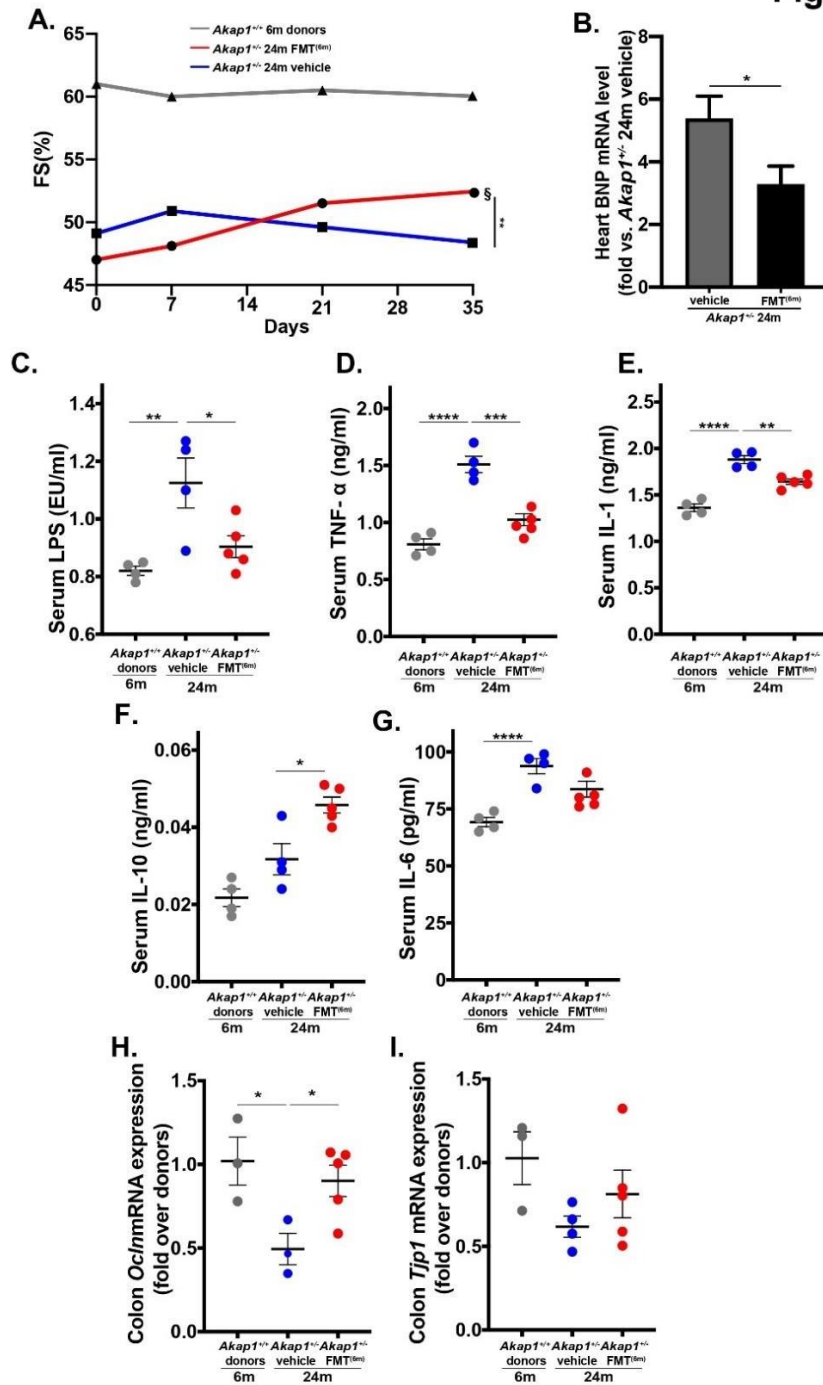
Figure 12: Healthy FMT modulates cardiac disfunction, leaky gut and systemic inflammation. *Cumulative data from 6m Akap1⁺/⁺ donors, 24m Akap1⁺/⁻ FMT (6m) and 24m Akap1⁺/⁻ vehicle of: % fractional shortening from(A); mRNA levels of BNP in cardiac samples (B); Serum levels of TNF- α(C)), IL-1(D), IL6(E), LPS(F), IL-10(G); colon mRNA expression levels of, Ocln (H), Tjp1 (I). Results are presented as mean ± SEM. Statistical significances were assessed using multiple comparisons were made by two-way ANOVA with Tukey correction *p≤0.05, **p≤0.01, ***p≤0.001 ****≤0.0001).*

To clarify the contribution of gut microbiota to the cardiac and inflammation phenotype of *Akap1*^{+/-}, microbiota composition was assessed all experimental groups after a 5-week FMT, as descript in precedent chapter. Results of core microbiome analysis, sing linear discriminant analysis (LDA) combined with effect size (LEfSe), were obtained by comparing FMT-treated mice to the ones receiving vehicle (Fig. 13; 14; 15). We observed that specific taxa failed to engraft in transplanted mice, possibly due to host incompatibility or antibiotic effect, whereas others thrived. In Particular, statistical analysis showed that species *Helicobacter_apodemus* and *Peptococcaceae*, were significantly increased, in mice of Group 1 compared to Group 3, after FMT using 24m *Akap1*^{+/-} mice as feces donors (Fig. 13 B, C; Fig. 14 B, C). Moreover, *Rikenellaceae*_RC9_*gut_group* and *Helicobacter_mastomyrinus* was significantly increased in mice of Group 2 compared to Group 4. These bacterial species are distinctive of *Akap1*^{+/-} genotype, seeing as how shared among 24m *Akap1*^{+/-} donors and 6m, 24m *Akap1*^{+/+} recipient. (Fig. 13 A, B; Fig. 14 A, B). These conditions of dysbiosis have been both identified in acute myocardial ischemia and oxidative stress induced by High-Fat Diet[53,54].

After FMT using 6m *Akap1*^{+/+} as faces donors, microbiota analysis has showed that species *Mycoplasma* and *Lactobacillus* were reduced in Group 5, compared to Group 6 (Fig. 15). These species failed to be transplanted from 24m *Akap1*^{+/-} donors into groups 1 and 2.

FIGURE 13

A.

B.

Species	LDA score	p-value	24m *Akap1*⁺/⁺ vehicle	24m *Akap1*⁺/⁺ FMT (24m)
g__Muribaculaceae_s__uncultured_Bacteroidales	4.222	0.018	5.18%	1.83%
Muribaculum_intestinale	3.874	0.037	0.79%	0.11%
g__Lachnospiraceae_NK4A136_group___	4.100	0.028	3.00%	0.91%
Akkermansia_muciniphila	4.310	0.022	3.70%	0.01%
g__Odoribacter_s__uncultured_bacterium	3.749	0.043	0.17%	0.67%
g__Muribaculaceae_s__uncultured_Muribaculaceae	4.036	0.034	0.00%	0.30%
g__Muribaculaceae_s__unidentified	3.879	0.040	0.37%	1.47%
g__Rikenellaceae_RC9_gut_group_s__uncultured_organism	4.103	0.017	0.47%	2.44%
Helicobacter_mastomyrinus	4.105	0.017	0.68%	3.18%
f__Peptococcaceae_g__uncultured_s__unidentified	3.929	0.044	0.42%	1.77%

C.

Figure 13. *Gut microbiota differences based on 16S rDNA sequencing at genus and species taxonomic levels were identified using core microbiome analysis(A), linear discriminant analysis (LDA)combined with effect size (LEfSe) algorithm (B, C). In Panel (A), in red are marked the 15 species absent in Group 4 but shared among 24m Akap1⁺/⁻ donors and Groups 2, 6. In blue are marked the 6 species shared by 24m Akap1⁺/⁻ donors and Groups 2, but absent in Group 6. LDA scores (B) and relative abundance (C) of key phylotypes discriminating of Groups 2 and 4.*

FIGURE 14

A.

f__Desulfovibrionaceae;g__uncultured;s__uncultured_Desulfovibrioales
Helicobacter_apodemus
g__Rikenellaceae_RC9_gut_group;s__uncultured_organism
g__Desulfovibrio;s__Desulfovibrio_fairfieldensis
f__Bacteroidaceae;g__Bacteroides;__
f__Oscillospiraceae;g__uncultured;s__unidentified
f__Lachnospiraceae;g__uncultured;s__Clostridium_sp.
f__Lachnospiraceae;g__Blautia;

B.
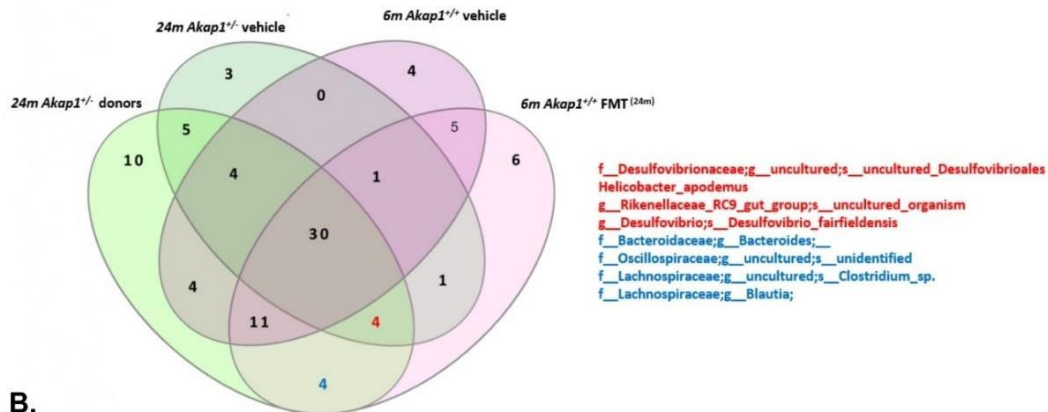
| Species	LDA score	p-value	6m *Akap1*+/+ vehicle	6m *Akap1*+/+ FMT (24m)
s__Helicobacter_apodemus	3.736	0.034	0.44%	1.52%
f__Peptococcaceae_g__uncultured_s__unidentified	3.490	0.037	0.25%	0.77%
s__Akkermansia_muciniphila	3.510	0.007	0.00%	0.53%
g__Muribaculaceae_s__uncultured_Muribaculaceae	3.305	0.037	0.55%	0.27%
g__Paraprevotella___	3.336	0.046	0.19%	0.09%
g__Lactobacillus___	3.228	0.049	0.20%	0.01%
g__[Eubacterium]_siraeum_group_s__uncultured_bacterium	3.440	0.022	0.50%	0.00%
o__Rhodospirillales_f__uncultured_g__uncultured___	3.235	0.022	0.18%	0.00%

C.
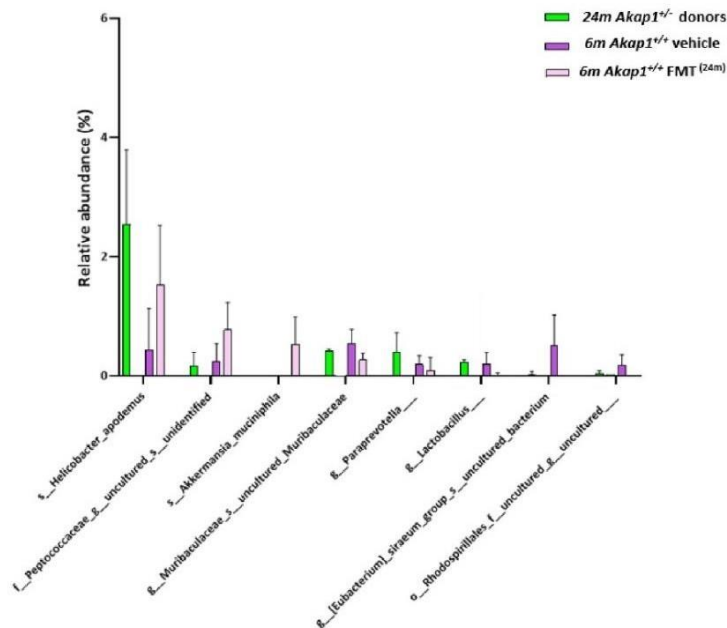
Figure 14: *Gut microbiota differences based on 16S rDNA sequencing at genus and species taxonomic levels were identified using core microbiome analysis(A), linear discriminant analysis (LDA)combined with effect size (LEfSe) algorithm (B, C). In Panel (A), in red are marked the 4 species absent in Group 3 but shared among 24m Akap1*+/-* donors and Groups 1, 6. In blue are marked the 4 species shared by 24m Akap1*+/-* donors and Group 1 but absent in Groups 3 and 6. LDA scores (B) and relative abundance (C) of key phylotypes discriminating of Groups 1 and 3.*

34

FIGURE 15

A.

f__Oscillospiraceae;g__uncultured;s__uncultured_bacterium
g__Mucispirillum;s__Mucispirillum_sp.
g__Paraprevotella;__
s__Burkholderiales_bacterium
g__Lachnospiraceae_NK4A136_group;s__uncultured_bacterium
g__Desulfovibrio;s__uncultured_bacterium
s__Bacteroides_caecimuris
f__Oscillospiraceae;g__Colidextribacter;__
g__Oscillibacter;s__Oscillibacter_sp.
f__Rikenellaceae

B.
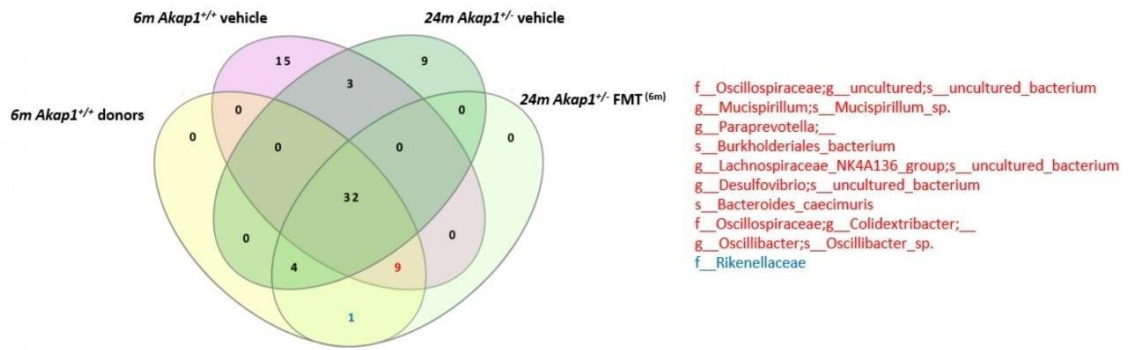
| Species	LDA score	p-value	24m Akap1+/- FMT (6m)	24m Akap1+/- vehicle
s__uncultured_Desulfovibrionales	3.735	0.020	0.36%	0.06%
f__Peptococcaceae_g__uncultured_s__unidentified	3.797	0.036	1.11%	0.23%
_g__Muribaculaceae_s__uncultured_Bacteroidales	4.142	0.016	1.58%	4.19%
f__Muribaculaceae_g__Muribaculaceae_s__unidentified	3.923	0.010	0.75%	2.20%
g__Lactobacillus___	3.904	0.028	0.14%	1.40%
g__Mycoplasma___	3.973	0.007	0.00%	1.41%
g__Candidatus_Arthromitus_s__uncultured_bacterium	3.640	0.049	0.01%	0.34%

C.
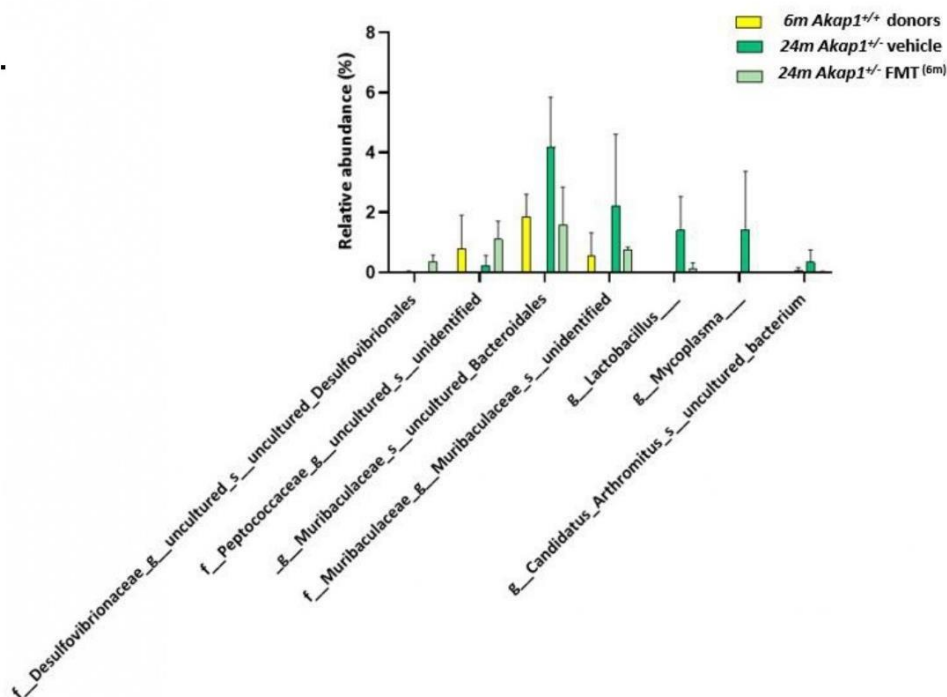
Figure 15: *Gut microbiota differences based on 16S rDNA sequencing at genus and species taxonomic levels were identified using core microbiome analysis(A), linear discriminant analysis (LDA)combined with effect size (LEfSe) algorithm (B, C). In Panel (A), in red are marked the 9 species absent in Group 6 but shared among 6m Akap1+/+ donors and Groups 5, 3. In blue are marked the 1 specie shared by 6m Akap1+/+ donors and Group 5 but absent in Groups 6 and 3. LDA scores (B) and relative abundance (C) of key phylotypes discriminating of Groups 5 and 6.*

35

Part IV

Discussion and Conclusion

Discussion

Transverse aortic constriction induces gut barrier alterations, microbiota remodeling and systemic inflammation.

Several studies have demonstrated that patients with HF display alterations of villi shape in intestinal mucosa resulting in intramucosal acidosis[55,56] and intestinal wall thickness. Moreover, alterations in gut microbial communities have been reported in patients with HF[57,58]. In this study we demonstrated that gut hypoperfusion induced by TAC was associated to a prompt and strong weakening of intestinal barrier integrity, decrease of colon anti-inflammatory cytokine levels, increase of serum levels of LPS and proinflammatory cytokines, and significant differences in gut microbiota.

As descript previously, TAC was associated with a prompt reduction in abdominal aortic blood flow and intestinal hypoperfusion, accompanied by a rapid impairing of gut barrier structure as demonstrated by reduction of ZO-1 and *Ocln* levels and increased FITC-dextran translocation across intestinal epithelium into blood. Moreover, we concurrently found a significant increase of LPS and proinflammatory cytokines in systemic blood circulation of TAC mice compared to sham. Of note, together with remarkable inflammatory infiltrate persistence and high levels of inflammatory markers, gut barrier was still functionally compromised in TAC 4w mice, as revealed by FITC-dextran *in vivo* permeability assay, despite a recovery of tight junctions mRNA and proteins levels at this time point. We cannot exclude that at later time points gut barrier function could be restored.

Our results demonstrate the murine model of TAC induces differences in fecal bacterial genera inside *Actinobacteria*, *Firmicutes*, *Proteobacteria* and TM7 phyla. These dramatic alterations of gut microbiota were associated to hypoperfusion induced by TAC surgery. Based on LEfSE results, taxa correlated to dysbiosis and colonic inflammation, such as F16, significantly increased after TAC[59,60]. Furthermore, we identified unclassified genus of RF32 (*Proteobacteria phylum*) as a potential microbial biomarker and source of LPS in TAC operated mice, possibly contributing to colonic inflammation. Moreover, in TAC 4w mice gut microbiota was characterized by an increase in genera *Turicibacter* and *Lactobacillus*. The increase of these lactate-producing bacteria (namely *T. sanguinis* and *L. frumenti*, according to species-level SPINGO classification) concurred with the depletion of butyrate-producing bacteria (genus *Oscillospira*, taxonomically classified as *P. capillosus* and *F. plautii* species after SPINGO procedure) in TAC mice, and these results were also corroborated by PICRUST analysis. Recent studies have implicated increases in genus Lactobacillus in pathophysiology of cardiovascular diseases, even if conflicting results have been reported in HF. Increases in

lactate-producing Lactobacillus have been demonstrated in elderly patients with HF and in animal models of hypertension[61,62]. Consistently, ST-segment elevation myocardial infarction (STEMI) patients were characterized by increased circulating levels of intestinal Lactobacilli, associated with systemic inflammation and adverse cardiovascular events[61]. On the contrary, ferulic acid administration, which improves cardiac function in TAC mice, has been shown to increase intestinal Lactobacillus[63]. Moreover, a reduction of Lactobacillus has been reported in gut microbiota of rats with isoproterenol-induced HF[64]. Thus, further investigations will be necessary to clarify the role of Lactobacillus phylotypes in the pathophysiology of HF, ideally with species-level approaches.

Mitochondrial a Kinase Anchor Proteins in cardiovascular health and disease

Previous studies in our laboratory and others have shown the crucial role of mitochondrial AKAPs in the regulation of several cardiovascular functions under physiological or pathological conditions, suggesting that these signaling hubs represent novel and druggable targets for multiple cardiovascular diseases. To obtain specific inhibition of mitochondrial AKAPs in the cardiovascular system, several aspects should be considered. Since AKAPs lack intrinsic enzymatic activity and function as nucleators of signalosomes at specific cellular locations in some cases with still unknown cardiovascular functions several different strategies could be potentially undertaken to modulate AKAP levels, mitochondrial targeting and/or selective interactions with effectors. Accumulating evidence identifies subcellular cAMP signaling as the main contributor of cardiomyocyte homeostasis. Consequently, disruption of microdomains of cAMP triggers cardiomyocyte dysfunction, promoting CVD. With their role in regulating local cAMP signaling, mitochondrial AKAPs are uniquely positioned to modulate mitochondrial function and, in general, cellular bioenergetics in cellular health and disease. Moreover, the use of global activators or inhibitors of cAMP/PKA signaling to indiscriminately affect all compartmentalized intracellular pools of cAMP, overexpression or silencing of specific AKAPs with a mechanistic role in specific physiological or pathological conditions may represent valuable approaches to restrict spatial regulation of AKAPs signaling. Future studies to unravel mechanisms of mitochondrial AKAPs function in CVD holds great basic and, potentially, clinical potential.

Partial loss of *Akap1* gene promotes cardiac dysfunction, gut barrier abnormalities, and alteration of gut microbiota composition during ageing.

Data reported in this part of the thesis demonstrate that AKAP1 plays a role in cardiomyocyte

hypertrophy and development of cardiac dysfunction during aging, as demonstrated reduced FS%, an increase in cardiomyocytes and an increase in the fibrotic area of LV in $Akap1^{+/-}$ old age mice. As previously descript, AKAP1 regulates ROS production and cardiomyocyte survival and commonly know there is a correlation between oxidative stress and dysbiosis[5]. In this study we confirmed that AKAP1 modulate intestine permeability, as shown by reduction of mRNA expression of ZO-1 and $Ocln$ levels and increased FITC-dextran translocation across intestinal epithelium into blood. Moreover, we concurrently found a significant increase of LPS and proinflammatory cytokines in systemic blood circulation of 24m $Akap1^{+/-}$ mice compared to $Akap1^{+/+}$ same age. Microbiota analysis reveal changes in bacterial populations during aging, in particular 24m $Akap1^{+/-}$ mice, showed an increase $Ruminococcus$ $Torques$ and a significant reduction of $Blautia\_producta$. $Ruminococcus$ $Torques$ participate in mucus degradation and gut barrier dysfunction[50], while $Blautia\_producta$ can produce butyric acid which has anti-inflammatory properties[51]. This condition of dysbiosis contributes to altered intestinal permeability with an increase in systemic inflammation.

The role played by AKAP1 in the gut-heart axis during aging has been corroborated by FMT studies. This experimental approach has allowed to modulate the composition of the intestinal microbiota and to understand the role of the latter in aging and in the development of cardiac dysfunction in relation to the partial deletion $Akap1$ gene. Our data show that FTM using 24m $Akap1^{+/-}$ mice as donors caused reduction of %FS, increase intestinal permeability and systemic inflammation in 6m and 24m $Akap1^{+/+}$ mice compared to vehicle-treated mice. Conversely, FMT using 6m $Akap1^{+/+}$ mice as donors induced in 24m $Akap1^{+/-}$ an improvement in %FS and intestinal permeability, with consequent reduced systemic inflammation compared to vehicle-treated mice.

Upon FMT treatment from 24m $Akap1^{+/-}$ donors, significant changes were detected in relative abundance of specific bacterial species between the recipient groups. In particular, harmful bacterial species as $Helicobacter$ $mastomyrinus,$ $Helicobacter\_apodemus$, $Peptococcaceae$ and $Rikenellaceae$ RC9 gut $group$ $species,$ were transplanted in 6m and 24m $Akap1^{+/+}$ mice from 24m $Akap1^{+/+}$ mice. Recent studies have demonstrated that $Helicobacter$ $mastomyrinus$ and $Helicobacter\_apodemus$ are associated colon inflammation[65,66], while $Peptococcaceae$ and $Rikenellaceae$ RC9 gut $group$ $specie$ are associated acute myocardial ischemia and oxidative stress induced by High-Fat Diet[53,54]. In reverse, after FMT treatment from 6m $Akap1^{+/+}$ donors, harmful bacterial species as $Lactobacillus$ and $Mycoplasma$ were reduced in 24m $Akap1^{+/-}$ recipient mice compared to vehicle. $Mycoplasma$ modulate colon inflammation[67], while $Lactobacillus$ is associated pathophysiology of cardiovascular diseases[61,62]

In conclusion, we demonstrated that partial deletion A*kap1* gene plays a crucial role on the gut-heart axis during aging, and that the manipulation of gut microbiota composition can modulate cardiac function, suggesting mitochondrial AKAPs play a fundamental role in controlling of ROS production and consequently the reduction of AKAP1 levels promote cardiac dysfunction, systemic inflammation and intestinal dysbiosis, during aging. The molecular mechanisms of how AKAP1 affects gut-heart axis homeostasis are currently unknown, future studies aimed at identifying pathways modulated by AKAP1 in the gut-heart axis will be critical to identify new possible molecular targets to restore levels of AKAP1, slowing cardiac senescence and improving the quality of life of patients with CVD.

Conclusions

In this long-lasting research journey, we investigated the effects and role of gut barrier permeability, microbiota remodeling and systemic inflammation, in murine models of pressure overload, and the role of mitochondrial AKAP1 in cardiovascular senescence, systemic inflammation, gut barrier permeability and microbiota remodeling by fecal microbiota transplantation. All our results suggest that gut microbiota play a critical physiological and metabolic role as mediator of gut-heart crosstalk. Future studies, aiming at identification of bacterial metabolites, which involve numerous microbial pathways implicated in the pathogenesis of CVD disorders, could be fundamental identification for potential biomarkers for diagnosis and treatment.

Bibliography

1. Bisaccia, G., Ricci, F., Gallina, S., Di Baldassarre, A. & Ghinassi, B. Mitochondrial Dysfunction and Heart Disease: Critical Appraisal of an Overlooked Association. *Int J Mol Sci* **22**, (2021).

2. Chistiakov, D. A., Shkurat, T. P., Melnichenko, A. A., Grechko, A. V & Orekhov, A. N. The role of mitochondrial dysfunction in cardiovascular disease: a brief review. *Ann Med* **50**, 121–127 (2018).

3. Paolillo, R. *et al.* Mitochondrial a Kinase Anchor Proteins in Cardiovascular Health and Disease: A Review Article on Behalf of the Working Group on Cellular and Molecular Biology of the Heart of the Italian Society of Cardiology. *Int J Mol Sci* **23**, (2022).

4. Wang, L. *et al.* The role of the gut microbiota in health and cardiovascular diseases. *Molecular biomedicine* **3**, 30 (2022).

5. Duan, C. *et al.* Activated Drp1-mediated mitochondrial ROS influence the gut microbiome and intestinal barrier after hemorrhagic shock. *Aging* **12**, 1397–1416 (2020).

6. Harikrishnan, S. Diet, the Gut Microbiome and Heart Failure. *Card Fail Rev* **5**, 119–122 (2019).

7. Schiattarella, G. G. *et al.* Gut microbe-generated metabolite trimethylamine-N-oxide as cardiovascular risk biomarker: a systematic review and dose-response meta-analysis. *Eur Heart J* **38**, 2948–2956 (2017).

8. Schiattarella, G. G., Sannino, A., Esposito, G. & Perrino, C. Diagnostics and therapeutic implications of gut microbiota alterations in cardiometabolic diseases. *Trends Cardiovasc Med* **29**, 141–147 (2019).

9. Forkosh, E. & Ilan, Y. The heart-gut axis: new target for atherosclerosis and congestive heart failure therapy. *Open Heart* **6**, e000993 (2019).

10. Kelley, E. E., Modest, E. J. & Burns, C. P. Unidirectional membrane uptake of the ether lipid antineoplastic agent edelfosine by L1210 cells. *Biochem Pharmacol* **45**, 2435–2439 (1993).

11. Ott, S. J. *et al.* Detection of Diverse Bacterial Signatures in Atherosclerotic Lesions of Patients With Coronary Heart Disease. *Circulation* **113**, 929–937 (2006).

12. Qin, J. *et al.* A metagenome-wide association study of gut microbiota in type 2 diabetes. *Nature* **490**, 55–60 (2012).

13. Tang, W. H. W., Kitai, T. & Hazen, S. L. Gut Microbiota in Cardiovascular Health and Disease. *Circ Res* **120**, 1183–1196 (2017).

14. Tang, W. H. W., Li, D. Y. & Hazen, S. L. Dietary metabolism, the gut microbiome, and heart failure. *Nat Rev Cardiol* **16**, 137–154 (2019).

15. Perrino, C. Intermittent pressure overload triggers hypertrophy-independent cardiac dysfunction and vascular rarefaction. *Journal of Clinical Investigation* **116**, 1547–1560 (2006).

16. Schaper, J. *et al.* Impairment of the myocardial ultrastructure and changes of the cytoskeleton in dilated cardiomyopathy. *Circulation* **83**, 504–514 (1991).

17. Forte, M. *et al.* The role of mitochondrial dynamics in cardiovascular diseases. *Br J Pharmacol* **178**, 2060–2076 (2021).

18. Perrino, C. & Rockman, H. A. Reversal of cardiac remodeling by modulation of adrenergic receptors: a new frontier in heart failure. *Curr Opin Cardiol* **22**, 443–449 (2007).

19. Rockman, H. A., Koch, W. J. & Lefkowitz, R. J. Seven-transmembrane-spanning receptors and heart function. *Nature* **415**, 206–12 (2002).

20. Wang, J., Gareri, C. & Rockman, H. A. G-Protein–Coupled Receptors in Heart Disease. *Circ Res* **123**, 716–735 (2018).

21. Ippolito, M. & Benovic, J. L. Biased agonism at β-adrenergic receptors. *Cell Signal* **80**, 109905 (2021).

22. Bond, R. A., Lucero Garcia-Rojas, E. Y., Hegde, A. & Walker, J. K. L. Therapeutic Potential of Targeting ß-Arrestin. *Front Pharmacol* **10**, 124 (2019).

23. Boularan, C. & Gales, C. Cardiac cAMP: production, hydrolysis, modulation and detection. *Front Pharmacol* **6**, (2015).

24. Lezoualc'h, F., Fazal, L., Laudette, M. & Conte, C. Cyclic AMP Sensor EPAC Proteins and Their Role in Cardiovascular Function and Disease. *Circ Res* **118**, 881–897 (2016).

25. Liu, Y., Chen, J., Fontes, S. K., Bautista, E. N. & Cheng, Z. Physiological and pathological roles of protein kinase A in the heart. *Cardiovasc Res* **118**, 386–398 (2022).

26. Dodge-Kafka, K. L., Langeberg, L. & Scott, J. D. Compartmentation of cyclic nucleotide signaling in the heart: the role of A-kinase anchoring proteins. *Circ Res* **98**, 993–1001 (2006).

27. Ercu, M. & Klussmann, E. Roles of A-Kinase Anchoring Proteins and Phosphodiesterases in the Cardiovascular System. *J Cardiovasc Dev Dis* **5**, 14 (2018).

28. Colombe, A.-S. & Pidoux, G. Cardiac cAMP-PKA Signaling Compartmentalization in Myocardial Infarction. *Cells* **10**, 922 (2021).

29. Carlucci, A., Lignitto, L. & Feliciello, A. Control of mitochondria dynamics and oxidative metabolism by cAMP, AKAPs and the proteasome. *Trends Cell Biol* **18**, 604–613 (2008).

30. Di Benedetto, G., Lefkimmiatis, K. & Pozzan, T. The basics of mitochondrial cAMP signalling: Where, when, why. *Cell Calcium* **93**, 102320 (2021).

31. Sherpa, R. T. *et al.* Mitochondrial A-kinase anchoring proteins in cardiac ventricular myocytes. *Physiol Rep* **9**, e15015 (2021).

32. Sung, J. Y. *et al.* WAVE1 controls neuronal activity-induced mitochondrial distribution in dendritic spines. *Proceedings of the National Academy of Sciences* **105**, 3112–3116 (2008).

33. Ould Amer, Y. & Hebert-Chatelain, E. Mitochondrial cAMP-PKA signaling: What do we really know? *Biochimica et Biophysica Acta (BBA) - Bioenergetics* **1859**, 868–877 (2018).

34. Merrill, R. A. & Strack, S. Mitochondria: A kinase anchoring protein 1, a signaling platform for mitochondrial form and function. *Int J Biochem Cell Biol* **48**, 92–96 (2014).

35. Liu, Y., Merrill, R. A. & Strack, S. A-Kinase Anchoring Protein 1: Emerging Roles in Regulating Mitochondrial Form and Function in Health and Disease. *Cells* **9**, (2020).

36. Marin, W. A-kinase anchoring protein 1 (AKAP1) and its role in some cardiovascular diseases. *J Mol*

Cell Cardiol **138**, 99–109 (2020).

37. Cardone, L. *et al.* A-kinase anchor protein 84/121 are targeted to mitochondria and mitotic spindles by overlapping amino-terminal motifs. *J Mol Biol* **320**, 663–75 (2002).

38. Carlucci, A. *et al.* Proteolysis of AKAP121 regulates mitochondrial activity during cellular hypoxia and brain ischaemia. *EMBO J* **27**, 1073–1084 (2008).

39. Kim, H. *et al.* Fine-Tuning of Drp1/Fis1 Availability by AKAP121/Siah2 Regulates Mitochondrial Adaptation to Hypoxia. *Mol Cell* **44**, 532–544 (2011).

40. Cardone, L. *et al.* Mitochondrial AKAP121 binds and targets protein tyrosine phosphatase D1, a novel positive regulator of src signaling. *Mol Cell Biol* **24**, 4613–26 (2004).

41. Livigni, A. *et al.* Mitochondrial AKAP121 Links cAMP and src Signaling to Oxidative Metabolism. *Mol Biol Cell* **17**, 263–271 (2006).

42. Schiattarella, G. G. *et al.* Loss of Akap1 Exacerbates Pressure Overload-Induced Cardiac Hypertrophy and Heart Failure. *Front Physiol* **9**, (2018).

43. Schiattarella, G. G. *et al.* Akap1 Deficiency Promotes Mitochondrial Aberrations and Exacerbates Cardiac Injury Following Permanent Coronary Ligation via Enhanced Mitophagy and Apoptosis. *PLoS One* **11**, e0154076 (2016).

44. Schiattarella, G. G. *et al. Akap1* Regulates Vascular Function and Endothelial Cells Behavior. *Hypertension* **71**, 507–517 (2018).

45. Perrino, C. *et al.* AKAP121 downregulation impairs protective cAMP signals, promotes mitochondrial dysfunction, and increases oxidative stress. *Cardiovasc Res* **88**, 101–110 (2010).

46. Perrino, C. *et al.* Dynamic Regulation of Phosphoinositide 3-Kinase-γ Activity and β-Adrenergic Receptor Trafficking in End-Stage Human Heart Failure. *Circulation* **116**, 2571–2579 (2007).

47. Wang, A. *et al.* Targeting mitochondria-derived reactive oxygen species to reduce epithelial barrier dysfunction and colitis. *Am J Pathol* **184**, 2516–27 (2014).

48. Vancamelbeke, M. & Vermeire, S. The intestinal barrier: a fundamental role in health and disease. *Expert Rev Gastroenterol Hepatol* **11**, 821–834 (2017).

49. Ahmad, A. F., Ward, N. C. & Dwivedi, G. The gut microbiome and heart failure. *Curr Opin Cardiol* **34**, 225–232 (2019).

50. Naik, S. S. *et al.* Association of Gut Microbial Dysbiosis and Hypertension: A Systematic Review. *Cureus* **14**, e29927 (2022).

51. Fang, C. *et al.* Dysbiosis of Gut Microbiota and Metabolite Phenylacetylglutamine in Coronary Artery Disease Patients With Stent Stenosis. *Front Cardiovasc Med* **9**, 832092 (2022).

52. Citraro, R. *et al.* First evidence of altered microbiota and intestinal damage and their link to absence epilepsy in a genetic animal model, the WAG/Rij rat. *Epilepsia* **62**, 529–541 (2021).

53. Sun, L. *et al.* Cecal Gut Microbiota and Metabolites Might Contribute to the Severity of Acute Myocardial Ischemia by Impacting the Intestinal Permeability, Oxidative Stress, and Energy Metabolism. *Front Microbiol* **10**, (2019).

54. Wang, B. *et al.* A High-Fat Diet Increases Gut Microbiota Biodiversity and Energy Expenditure Due to Nutrient Difference. *Nutrients* **12**, 3197 (2020).

55. Maynard, N. Assessment of Splanchnic Oxygenation by Gastric Tonometry in Patients With Acute Circulatory Failure. *JAMA: The Journal of the American Medical Association* **270**, 1203 (1993).

56. Krack, A. *et al.* Studies on intragastric PCO $_2$ at rest and during exercise as a marker of intestinal perfusion in patients with chronic heart failure. *Eur J Heart Fail* **6**, 403–407 (2004).

57. Sandek, A. *et al.* Intestinal Blood Flow in Patients With Chronic Heart Failure. *J Am Coll Cardiol* **64**, 1092–1102 (2014).

58. Sandek, A. *et al.* Altered Intestinal Function in Patients With Chronic Heart Failure. *J Am Coll Cardiol* **50**, 1561–1569 (2007).

59. Kuehbacher, T. *et al.* Intestinal TM7 bacterial phylogenies in active inflammatory bowel disease. *J Med Microbiol* **57**, 1569–1576 (2008).

60. Carvalho, R. *et al.* Gut microbiome modulation during treatment of mucositis with the dairy bacterium Lactococcus lactis and recombinant strain secreting human antimicrobial PAP. *Sci Rep* **8**, 15072 (2018).

61. Zhou, X. *et al.* Gut-dependent microbial translocation induces inflammation and cardiovascular events after ST-elevation myocardial infarction. *Microbiome* **6**, 66 (2018).

62. Kamo, T. *et al.* Dysbiosis and compositional alterations with aging in the gut microbiota of patients with heart failure. *PLoS One* **12**, e0174099 (2017).

63. Liu, Z. *et al.* Ferulic acid increases intestinal Lactobacillus and improves cardiac function in TAC mice. *Biomedicine & Pharmacotherapy* **120**, 109482 (2019).

64. Zheng, A. *et al.* Changes in Gut Microbiome Structure and Function of Rats with Isoproterenol-Induced Heart Failure. *Int Heart J* **60**, 1176–1183 (2019).

65. Chai, J. N. *et al. Helicobacter* species are potent drivers of colonic T cell responses in homeostasis and inflammation. *Sci Immunol* **2**, (2017).

66. Eaton, K. A., Opp, J. S., Gray, B. M., Bergin, I. L. & Young, V. B. Ulcerative typhlocolitis associated with Helicobacter mastomyrinus in telomerase-deficient mice. *Vet Pathol* **48**, 713–25 (2011).

67. Tang, S. *et al.* Chronic heat stress induces the disorder of gut transport and immune function associated with endoplasmic reticulum stress in growing pigs. *Anim Nutr* **11**, 228–241 (2022).

Stefania D'Apice

Date of birth: 12/04/1992 | **Nationality:** Italian | **Gender:** Female | **Phone number:** (+39) 3389138623 (Mobile) | **Email address:** ste.dapice@gmail.com |

Address: Via Andolfi 77, 80058, Torre Annunziata, Italy (Home)

WORK EXPERIENCE

30/09/2019 – CURRENT
PHD STUDENT DEPARTMENT OF "ADVANCED BIOMEDICAL SCIENCES" OF THE UNIVERSITY OF NAPLES "FEDERICO II"

International PhD Programme in Cardiovascular Pathophysiology and Therapeutics. Tutor: Prof.ssa Perrino Cinzia

06/05/2019 – 06/11/2019
BIOLOGIST DEPARTMENT OF "ADVANCED BIOMEDICAL SCIENCES" OF THE UNIVERSITY OF NAPLES "FEDERICO II"

Scholarship holder at the molecular cardiology laboratory of the Department of Advanced Biomedical Sciences, University of Naples Federico II. Prof. Giovanni Esposito.
Evaluation of the role of DNA repair and the role of the protein behind the activation of DNA damage repair processes, known as ATM, at Cardiac level.

Address Napoli, Italy

10/2017 – 11/2018
BIOLOGIST DEPARTMENT OF "ADVANCED BIOMEDICAL SCIENCES" OF THE UNIVERSITY OF NAPLES "FEDERICO II"

Training internship at the molecular cardiology laboratory of the Advanced Biomedical Sciences Department of the University of Naples Federico II. Prof. Cinzia Perrino.

Study of the main molecular mechanisms involved in cardiovascular diseases in animal and cellular models.

Address Napoli, Italy

16/04/2016 – 16/10/2016
BIOLOGIST DOTT.SSA DI COSTANZO ANNA

Execution of biochemical-clinical analyzes on blood, serum, plasma and biological fluids.

Business or Sector Professional, scientific and technical activities |

Address Via Luigi Oliva, 80041, Boscoreale (Na), Italy

EDUCATION AND TRAINING

23/11/2018 Napoli, Italy
MASTER'S DEGREE IN BIOLOGICAL SCIENCES University of Naples Federico II

Grade: 110/110 cum laude

Address Napoli, Italy

15/06/2017 Napoli, Italy
MASTER IN FOOD HYGIENE, NUTRITION AND WELLNESS University of Naples "Federico II"

Address Napoli, Italy

17/02/2016 Napoli, Italy
BACHEROL'S DEGREE IN BIOLOGICAL SCIENCES University of Naples Federico II

Grade: 92/110

Address Napoli, Italy

05/07/2011 Nocera Inferiore (Sa), Italy
HIGH SCHOOL DIPLOMA PSYCHO-PSYCHO-PEDAGOGICAL MATURITY Liceo A. Galizia

Grade: 74/100

Address Nocera Inferiore (Sa), Italy

LANGUAGE SKILLS

Mother tongue(s):   **ITALIAN**

Other language(s):

	UNDERSTANDING		SPEAKING		WRITING
	Listening	Reading	Spoken production	Spoken interaction	
ENGLISH	B2		B2	B2	

Levels: A1 and A2: Basic user; B1 and B2: Independent user; C1 and C2: Proficient user

DIGITAL SKILLS

Microsoft Office | Zoom | Social Media | Microsoft Word | Google Drive | Microsoft Excel | MS Office (Word Excel PowerPoint) | Skype | Gmail

ADDITIONAL INFORMATION

COMMUNICATION AND INTERPERSONAL SKILLS

Communication and interpersonal skills Excellent communication and relational skills in the workplace, to work in a team and reach a common municipality

JOB-RELATED SKILLS

Job-related skills

Biochemical-clinical analysis techniques:
-**Microbiology**: preparation of culture media, seeding and isolation and identification of bacterial cells, antibiogram;
Physical-chemical analysis of urine and observation of sediments under an optical microscope;
-**Hemocoagulation**: hemochromes, PT, PTT, fibrinogen, blood group identification;
-**Clinical chemistry**: use of IL600 analyzer;
-**Immunometry**: use of LIASON, IMMULITE200 and VIDAS analyzers;
-**Istology**: preparation of tissue sections for observation under an optical microscope and fluorescence microscope;
Molecular Biology and Biochemistry techniques:
-PCR, Real-Time PCR, Western Blotting;
 -Experience study cardiovascular disease in mice model : surgical, echocardiography and cardiomyocyte extraction

SCIENTIFIC PUBLICATION

Scientific Publication

Mitochondrial a Kinase Anchor Proteins in Cardiovascular Health and Disease: A Review Article on Behalf of the Working Group on Cellular and Molecular Biology of the Heart of the Italian Society of Cardiology. Int J Mol Sci 2022 Jul 12;23(14):7691. PMID: 35887048

Transverse aortic constriction induces gut barrier alterations, microbiota remodeling and systemic inflammation. Sci Rep. 2021 Apr 1;11(1):7404 PMID:33795775

Lights and shadows of combined epigenomic and transcriptomic profiling to identify novel diagnostic, prognostic or therapeutic targets for cardiovascular diseases Giornale italiano di medicina del lavoro ed ergonomia.2019 Dec;41(4):328-332. PMID:32126603

Loss of Akap1 Exacerbates Pressure Overload-Induced Cardiac Hypertrophy and Heart Failure. Front Physiol. 2018 May 28;9:558. PMID:29892230

CONFERENCES AND SEMINARS

Società Italiana di cardiologia 83° Edizione SIC
mitoAKAPs play a role in the progression towards heart failure modulating gut integrity and composition during aging D'Apice S, Paolillo R, Coretti L, Lama A, Boccella N, Mollica MP, Esposito G, Lembo F, Perrino C

Società Italiana di cardiologia 83° Edizione SIC
Ataxia Telangiectasia Mutated protein modulates glucose and lipid metabolism in the heart Paolillo R, Caterino M, D'Apice S, PhD; Pezone A, Boccella N, Pirozzi M, Coppola L, Gentile A , Lombardi A, Esposito G, Ruoppolo M, Avvedimento, Perrino C

American Heart Association congress AHA November 2022
Impaired Mitochondrial Quality Control Drives the Development of Cardiomyopathy in Anderson-Fabry Disease Jessica Gambardella, Antonella Fiordelisi, Roberta Avvisato, Federica A Cerasuolo, Antonietta Buonaiuto, Nella Prevete, Cinzia Perrino, Valeria D'Argenio, Roberta Paolillo, Stefania D'Apice, Gaetano Santulli, Daniela Sorriento, Guido Iaccarino

società italiana dell'ipertensione arteriosa SIIA 2022
The selective deletion of tyrosyne hydroxylase gene in the endothelium affects cardiovascular function Antonella Fiordelisi , Jessica Gambardella , FedericaAndrea Cerasuolo , Roberta Avvisato , Roberta Paolillo , Stefania D'Apice , Cinzia Perrino , Michele Ciccarelli , Guido Iaccarino , Daniela Sorriento

European Society of Cardiology ESC 2021
Partial loss of Akap1 promotes cardiac dysfunction, gut barrier dysfunction and alterations of gut microbiota composition during aging D'Apice S, Paolillo R, Boccella N, Coretti L, Lama A, Avvedimento M, Esposito G, Lembo F, Perrino C

European Society of Cardiology ESC 2021
Small nucleolar RNA SNORD3A: a potential new biomarker and molecular player in heart failure Roberta Paolillo, Giacomo Gabriele Schiattarella, Stefania D'Apice, Christopher Holley, Alessandro Della Corte, Ciro Bancone, Cinzia Perrino, Giovanni Esposito

Acknowledgments

I would like to express my gratitude to my Promotor, Prof. Perrino Cinzia who assisted and guided me throughout this project and for always encouraging to improve my scientific achievements.

I would also like to thank Prof. Esposito Giovanni who supported me and gave me the chance to work in his research laboratory for all these years.

I would like to thank my co-Promotor Dr. Coretti Lorena for all help and scientific collaboration advice for this thesis.

I would like to thank the coordinator Prof. Izzo Raffaele and all Cardiophat PhD program for the studentship that allowed me to obtain the PhD title.

I wish to thank all my colleagues that I met during this experience for all the help provided.

I would like to thank my husband Nunzio for the constant support and encouragement; this goal would have not been possible without him. Moreover, I would like thanks my wonderful daughter Annalisa, for bringing joy into my life. In finally, I would like to thank all my family for the support and love that they give me.